Received: 7 April 2020 | Revised: 10 December 2020 | Accepted: 15 December 2020

DOI: 10.1111/jzs.12453

JOURNAL OF ZOOLOGICAL SYSTEMATICS AND EVOLUTIONARY RESEARCH — WILEY

ORIGINAL ARTICLE

Systematic review of the polychromatic ground snakes *Atractus snethlageae* complex reveals four new species from threatened environments

Paulo R. Melo-Sampaio[1] | **Paulo Passos**[1] | **Ana L.C. Prudente**[2] | **Pablo J. Venegas**[3] | **Omar Torres-Carvajal**[4]

[1]Departamento de Vertebrados, Museu Nacional, Universidade Federal do Rio de Janeiro, São Cristóvão, Rio de Janeiro, Brazil

[2]Laboratório de Herpetologia, Coordenação de Zoologia, Museu Paraense Emílio Goeldi, Belém, Pará, Brazil

[3]División de Herpetología, Centro de Ornitología y Biodiversidad (CORBIDI), Huertos de San Antonio, Surco, Lima, Peru

[4]Museo de Zoología, Escuela de Ciencias Biológicas, Pontificia Universidad Católica del Ecuador, Apartado, Quito, Ecuador

Correspondence
Paulo Roberto Melo-Sampaio, Departamento de Vertebrados, Museu Nacional, Universidade Federal do Rio de Janeiro, São Cristóvão, Rio de Janeiro, Brazil.
Email: prmelosampaio@gmail.com

Funding information
Conselho Nacional de Desenvolvimento Científico e Tecnológico, Grant/Award Number: 302611/2018-5, 306227/2015-0, 309560/2018-7, 439375/2016-9 and 440413/2015-0; Fundação Carlos Chagas Filho de Amparo à Pesquisa do Estado do Rio de Janeiro, Grant/Award Number: E-26/202.737/2018; Secretaría de Educación Superior, Ciencia, Tecnología e Innovación; Coordenação de Aperfeiçoamento de Pessoal de Nível Superior, Grant/Award Number: 88882.183267/2018-01

Abstract

We review the *Atractus snethlageae* species complex based on the examination of 330 specimens throughout its entire distribution, including its type series. We re-define *A. snethlageae* and recognize four new species previously assigned to it in the literature and natural history collections. Two of them are diagnosed through both phenotypic (meristic, morphometric, color pattern, and male genital structure) and molecular (phylogeny) evidence, while the other two are recognized on the basis of morphological characters only. We show that some Amazonian lowland species have more restricted ranges. The area covering the eastern portion of the state of Pará and western portion of the state of Maranhão in Brazil harbors restricted endemism for *Atractus*. This biogeographically important region is also the most threatened within Amazonia. Finally, we discuss the expected changes in the taxonomy of ground snakes with more robust hypotheses based on well-sampled phylogenies.

KEYWORDS
Amazonia, Andes, endemism, hemipenis, molecular phylogeny

1 | INTRODUCTION

The tree of life is being pruned by human activities at an unprecedented rate (Pimm et al., 2014). Habitat loss and species extinction are alarming issues worldwide, especially in the Neotropical region, where the largest continuous tropical forests and one of the most diverse biotas occur (Wilson, 1988). High rates of extinction (hundreds to millions of species) are expected in forthcoming years being surpassed only by catastrophic events (Pimm et al., 2014). In recent years, many species have been described from the Amazonian lowlands to the Tropical Andes (Blackburn et al., 2019). These intrinsically connected ecosystems are ranked among the likely to lose most vertebrates as a result of current deforestation rates (Scheffers et al., 2019). To make this bleak scenario even worse, many species including reptiles have suffered with unprecedent extinction rates in the last century (Ceballos et al., 2015), mainly on the tropical ecosystems due to a combination of complex factors (Ferrer-Paris et al., 2019).

Contributing authors: Paulo Passos (atractus@gmail.com), Ana L.C. Prudente (prudente@museu-goeldi.br), Pablo J. Venegas (sancarranca@yahoo.es), Omar Torres-Carvajal (omartorcar@gmail.com)

ZooBank link: LSID: urn:lsid:zoobank.org:pub:1F5D67AD-6CA0-4E31-89C0-7C5EF4219B2E

Neotropical groundsnakes of the genus *Atractus* Wagler 1830 are the most diversified, species-rich, and taxonomically complex radiation of the suborder Serpentes (Passos et al., 2013). The genus comprises 143 currently recognized species (Uetz et al., 2020). However, many species remain known only from their type series or from geographically restricted regions (Passos et al., 2019). Consequently, some important aspects related to geographic, ontogenetic, sexual dimorphism, and population variation have not yet been properly documented (Passos et al., 2012). For that reason, the taxonomic status or species boundaries in some taxa remains unsatisfactorily evaluated (Passos et al., 2010), which is of special concern considering the high level of restricted endemism and polychromatism reported in *Atractus*.

Systematic and taxonomic studies on Neotropical reptiles are of great importance for their conservation. Twenty percent of Neotropical reptile species are threatened, with the same proportion catalogued as Data Deficient (Böhm et al., 2013). Moreover, species with restricted ranges (geographical or altitudinal), highly specialized diet (earthworms), and limited activity patterns (concentrated on daytime and twilight) are sensitive to local extinctions (Ceballos et al., 2015). A global evaluation of trade risk across the vertebrate tree of life pointed out the genus *Atractus* as potentially under highest-risk for trade in the near future to pet activity (Scheffers et al., 2019). Therefore, we must settle the Linnaean shortfall of this emblematic group of snakes in order to get a better picture of its diversity and species-level conservation status.

Although some species groups were proposed for the genus over time (Passos et al., 2013; Passos et al., 2010; Passos, Mueses-Cisneros, Lynch, & Fernandes, 2009; Passos et al., 2016; Savage, 1960), only the *A. elaps* and *A. roulei* groups have been, consistently, recovered as monophyletic through all phylogenetic hypotheses published to date (see Passos et al., in press). Taxonomic history of banded *Atractus* began with the description of *Brachyorrhos badius*, *B. flammigerus*, and *B. schach* from Guianan region by Boie (1827). Duméril et al. (1854) synonymized *B. flammigerus* and *B. schach* with *B. badius* until Hoogmoed (1980) rediscovered the types of *Atractus badius*, *A. flammigerus* and *A. schach*, resurrecting the latter two from the synonymy with *A. badius*. Later, Hoogmoed (1982) conceived a widespread distribution for *A. flammigerus*, including portions outside the Guiana Shield. Cunha and Nascimento (1983) described *Atractus flammigerus snethlageae* based on Brazilian specimens from north and south of the Amazon River. Cunha and Nascimento (1984) also reported additional specimens of *Atractus schach* from eastern Pará and western Maranhão states, Brazil. Subsequently, Vanzolini (1986a) listed *A. flammigerus snethlageae* in his "Addenda and Corrigenda" in the Catalogue of Neotropical Squamata. However, Vanzolini (1986b) considered *A. snethlageae* as a full species without further comments. Dixon and Soini (1986) reported on two specimens of *Atractus flammigerus* from the Iquitos region, and Duellman and Salas (1991) reported *A. flammigerus* from Cuzco Amazónico (northern and southern Peru, respectively). *Atractus snethlageae* has been reported from Rondônia State, Brazil (Ávila-Pires et al., 2009; Bernarde & Abe, 2006; Bernarde et al., 2012; Jorge-da-Silva, 1993; Marçal et al., 2011; Nascimento et al., 1988). Giraudo and Scrocchi (2000) re-identified as *A. snethlageae* a specimen previously identified as *A. badius* (Serié, 1915) and discussed its presence in Argentina. Silva-Haad (2004) provided the first record of *A. snethlageae* from Colombia, and Gonzales and Embert (2008) reported it from Manupiri, Pando, Bolivia. The name *Atractus badius* has been often used in reference to *A. snethlageae* throughout Amazonia (but see Passos et al., in press). Similarly, *A. snethlageae* has been repeatedly mistaken with *A. major* (Pérez-Santos & Moreno, 1988; Savage, 1960) or *A. flammigerus* (Dixon & Soini, 1986; Duellman, 2005). The difficulty in the correct assignment of the name *A. snethlageae* reflects the remarkable polychromatism of this species throughout its widespread distribution and the possible existence of a species complex (Schargel et al., 2013). Passos et al. (2017) restricted *A. flammigerus* to the Guiana Shield. More recently, Melo-Sampaio et al. (2019) revised the taxonomic status of populations previously associated with *A. schach* and *A. snethlageae*, restricting the distribution of the former to the Guiana Shield and recognizing three new species, of which two—*Atractus dapsilis* Melo-Sampaio, Passos, Fouquet, Prudente, & Torres-Carvajal and *A. trefauti* Melo-Sampaio, Passos, Fouquet, Prudente, & Torres-Carvajal—resemble *A. snethlageae* in general coloration.

Herein, we combine morphological analyses and molecular phylogenetics to test species boundaries within the *Atractus snethlageae* complex throughout its distribution. We analyze the largest dataset to date, including 330 specimens and 30 new tissue samples of *Atractus snethlageae* (sensu lato) from Bolivia, Brazil, Colombia, Ecuador, and Peru, comprising most of its range of distribution as reported in the literature.

2 | MATERIAL AND METHODS

2.1 | Molecular sampling, techniques, and selection of sequences

We gathered liver tissue samples from 30 specimens representing six species within *Atractus snethlageae* complex. These samples were obtained through loans or donations from the following institutions: Universidade Federal do Acre (UFAC-RB), Rio Branco, Brazil; Museu Nacional, Universidade Federal do Rio de Janeiro (MNRJ), Rio de Janeiro, Brazil; Museu Paraense Emílio Goeldi (MPEG), Belém, Brazil; Universidade Federal de Mato Grosso (UFMT-R), Cuiabá, Brazil; Laboratory of Herpetology (MTR) from the Universidade de São Paulo (USP), São Paulo, Brazil; Museo de Zoología de la Pontificia Universidad Católica del Ecuador (QCAZ), Quito, Ecuador; Museo de Zoología de la Universidad Tecnológica Indoamérica (MZUTI), Quito, Ecuador; Centro de Ornitología y Biodiversidad (CORBIDI), Lima, Peru; Museo de la Universidad de San Marcos (MUSM), Lima Peru; and Centre de Recherche de Montabo (CNRS), Cayenne, French Guiana, France.

We obtained nucleotide sequences from three mitochondrial genes, *ribosomal large subunit gene* (*16S*, 53 samples), *subunit IV of NADH dehydrogenase* (*ND4*, 36 samples), *cytochrome b* (*CYTB*, 42

samples), as well as three nuclear genes, *oocyte maturation factor mos* (*CMOS*, 42 samples), *neurotrophin-3* (*NT3*, 46 samples), and *recombination-activating gene 1* (*RAG1*, 45 samples). We extracted genomic DNA from tissue samples stored in absolute or 95% ethanol using a guanidinium isothiocyanate extraction protocol (see details in Torres-Carvajal & Hinojosa, 2020). We performed Polymerase Chain Reaction (PCR) amplification of gene fragments in a final volume of 25 μl reactions using 1X PCR Buffer (–Mg), 3 mM $MgCl_2$, 0.2 mM dNTP mix, 0.2 μM of each primer, 0.1 U/μl of Taq DNA Polymerase and 1 μl of extracted DNA. Primers and protocols are listed in Table S1. All amplified markers were obtained from the same voucher specimen to avoid problems inherent with chimeric sequences.

We analyzed polymerase chain reaction products on 1% agarose gels by horizontal electrophoresis (the target fragment size was estimated from molecular weight markers) using SYBR1 Safe (Invitrogen, Carlsbad, CA) staining, with a Molecular Imager1 Gel DocTM XR+ Imaging System (Bio-Rad, Hercules, CA). We treated amplified products with ExoSAP-IT (Affymetrix, Cleveland, OH) to remove remaining dNTPs and primers, as well as extraneous single-stranded DNA produced in the PCR. We performed double-stranded sequencing of the PCR products in both directions with Macrogen Inc. New sequences are presented in Table S2 and museum vouchers are housed at CORBIDI, MNRJ, MZUSP, QCAZ, and UFMT-R.

In addition, we obtained GenBank sequences for 33 outgroup species (Table S2), limiting our sampling to species for which we verified directly the identifications of the vouchers. Specimen MZUTI 5409 (ANF 2390) listed as *Atractus touzeti* (Arteaga et al., 2017) was re-identified. We also excluded sequences of distantly related species [*Atractus albuquerquei* Cunha & Nascimento, 1983, *A. reticulatus* (Boulenger, 1885), *A. trihedrurus* Amaral, 1926 and *Atractus zebrinus* (Jan, 1862)], without vouchers or locality data and separated the chimeras (terminals composed of sequences from different individuals or different species; Table S3) presented by Grazziotin et al. (2012), Pyron et al. (2013), Pyron et al. (2015), Figueroa et al. (2016), Pyron et al. (2016), and Arteaga et al. (2017).

2.2 | Phylogenetic analyses

We assembled and aligned the data in Mega 7.0 (Kumar et al., 2016) under default settings for the alignment program Clustal W (Thompson et al., 1994) and built a concatenated matrix (Data S1) using SequenceMatrix (Vaidya et al., 2011). We then selected the best-fit nucleotide substitution models and partitioning scheme simultaneously using PartitionFinder 2 (Lanfear et al., 2016) under the Bayesian Information Criterion (Sullivan & Joyce, 2005), after partitioning the matrix by gene (*16S*, *CYTB*, *CMOS*, *ND4*, *NT3*, *RAG1*) (Table S4). We analyzed the concatenated, partitioned matrix under a Bayesian inference method using MrBayes v3.2.1 (Ronquist et al., 2012). We chose this strategy because Montingelli et al. (2019) demonstrated the advantages of multiple information, where a concatenated matrix has an important role summarizing few phylogenetically informative sites from the nuclear loci and filling the gap between some non-overlapping taxon sampling; and even if contradictory, the phylogenetic signal of the concatenated nuclear loci will reduce the influence of the mitochondrial data. All parameters except topology and branch lengths were unlinked between partitions. Four independent runs, each with four MCMC chains, were set for 10 million generations each, sampling every 10,000 generations. We used Tracer v1.6 (available from http://beast.bio.ed.ac.uk/Tracer) to assess convergence, stationarity, and effective sample sizes (ESS > 200) of model parameters. We used LogCombiner 1.8.4 (Drummond et al., 2012) to summarize the runs. Of 4,000 resulting trees, 10% were discarded as "burn-in" from each run. We used the resultant trees to calculate posterior probabilities (PP) in a maximum clade credibility tree in TreeAnnotator v1.8.3 (Drummond et al., 2012). We edited and visualized the phylogenetic trees using FigTree v1.4.4 (Available in http://tree.bio.ed.ac.uk/software/figtree/). We also performed Maximum likelihood (ML) analyses on the partitioned dataset using RAXML (Stamatakis, 2014) under the GTRCAT approximation (Stamatakis et al., 2008). Support of nodes was assessed using the rapid-bootstrapping algorithm with 1000 non-parametric bootstraps. We considered the clades with posterior probability values >0.95 and ML bootstraps >70 as strongly supported.

2.3 | Morphology, species boundaries and presentation rationale

Terminology for cephalic shields follows Savage (1960) and Peters (1964), whereas ventral and subcaudal counts follow Dowling (1951). Condition of the loreal scale follows Passos et al. (2007). Measurements were taken with a Mitutoyo® digital caliper to the nearest 0.1 mm, except for snout–vent length (SVL) and tail length (TL), which were measured with a ruler to the nearest 1 mm. Measurements and descriptions of paired cephalic scales are strictly based on the left side of the head. We follow the definitions of Passos et al. (2016) for body marks (blotches, spots, and dots), which were counted separately on each side of the dorsum, and used the term "blotch" to refer to broad (two or more scales long and wide) dorsal marks located on the vertebral and paravertebral regions. Colors were described following the standard catalogue of Köhler (2012). We analyzed 330 specimens of banded *Atractus*. The sex of specimens was determined by verifying presence-absence of hemipenes through a ventral incision at the base of the tail, except when hemipenes had been previously everted. We examined maxillae in situ under a Luxeo 4Z (Labomed) stereoscope through a narrow latero-medial incision between the supralabials and the maxillary arch. After removing tissues covering the maxillary bone, we counted teeth and empty sockets. The method for preparation of preserved hemipenes was modified from Pesantes (1994) by replacing potassium hydroxide (KOH) with distilled water and filling the hemipenes with petroleum jelly (Passos et al., 2016). Terminology for hemipenial descriptions follows Dowling and Savage (1960) and Zaher (1999), with a few minor modifications based on Passos et al. (2016).

Data from additional specimens of *Atractus* previously examined are listed in Meneses-Pelayo and Passos (2019) and such studies included examination of nearly all types available for the genus *Atractus*. Nonetheless, we list in the "Species Account" the type specimens of the *Atractus snethlageae* complex, in addition to sympatric morphologically similar congeners listed in the Appendix 1. In addition to phylogenetic relationships, we consider unique diagnostic characters distinguishing a putative taxon from the others in the *A. snethlageae* complex as species delimitation criteria (de Queiroz, 2007). Notwithstanding, we search for concordance between the discrete and continuous characters. Since some features such as color patterns, morphometrics, and hemipenial morphology are likely uncorrelated with each other; the correspondence between these data sources might represent independent evidence for robust species boundaries (Passos et al., 2018).

The rationale along the species account includes detailed morphological comparisons following at least one of these four types of hierarchical levels of similarity or historical association: (a) species with close phylogenetic relationships, recovered along the present study; (b) sympatric or parapatric taxa presenting similar color pattern, scutelation and morphometric features; (c) phenotypically similar taxa even known to occur parapatrically or allopatrically regarding the *A. snethlageae* species complex (e.g., *A. schach* and closely related species; see Melo-Sampaio et al., 2019); (d) species previously confused with *A. snethlageae* in literature or scientific collections (e.g., *A. flammigerus*; see Passos et al., 2017). We follow Passos, Fernandes, et al. (2010) regarding conditions of morphological characters used in diagnoses and descriptions. All species recognized herein as monophyletic exhibited unambiguous phenotypic diagnostic characters or exclusive combinations of traits.

3 | RESULTS

3.1 | Phylogenetic analyses

Maximum Likelihood (ML) and Bayesian Inference (BI) trees are in agreement (Figure 1; Figures S1-S2). We recovered a paraphyletic *A. snethlageae* (sensu lato) in four distinct clades. A clade from Ecuador was recovered with maximum support in both trees as sister to a larger clade, containing Guianan clade (*Atractus dapsilis* (*A. schach*, *A. trefauti*)) as sister to clade containing the other three *A. snethlageae* (sensu lato) clades. A sample from southeastern Peru comprises a unique clade. A clade composed by eastern Amazonia specimens represented by Tocantins and Xingu river is nested with specimens from Madeira, Purus, and Aripuanã river in south Amazonia and Caxiuanã bay in eastern Amazonia. This clade is recognized as *Atractus snethlageae* sensu stricto. The last clade is composed of Peruvian and Ecuadorian specimens from populations adjacent to Amazonian slopes of Andes and the extreme western lowland Amazonian specimens. To better reflect the relationships among sampled populations and maintain species monophyly, we describe below three of the four clades of *A. snethlageae* (sensu lato) as separate species, each supported by putative autopomorphies or unique combinations of morphological characters.

3.2 | Phenotypic variation among different populations of *Atractus snethlageae*

We discovered two additional unnamed species upon examination of hemipenial morphology, maxillary dentition, morphometrics, coloration, and scale counts. In the absence of molecular data for these species, we compared them with geographically close and morphologically similar congeners according to our own delimitation criteria (see above).

Morphological comparisons with respect to the cis-Andean *Atractus* complexes, species groups or previously recovered clades south of the Amazon River: *A. schach* complex (including *A. snethlageae* and other allied species) differs from the *A. elaps* species group [except for *A. latifrons* (Günther, 1868)], *A. emmeli* (Boettger, 1888), *A. occiptoalbus* (Jan, 1862), *A. roulei* Depax, 1910 and *A. trilineatus* Wagler, 1828 groups or complexes of species (in parentheses) in having 17 dorsal scale rows (vs. 15 dorsal scale rows); from the *Atractus collaris* Peracca, 1897 group in lacking apical pits and supracloacal tubercles (vs. presence of apical pits in male and females, and supracloacal tubercles in sexually mature males); from the *A. elaps* (Günther, 1858) species group [including *A. latifrons* (Günther, 1868)] in having loreal scales twice as long as high and rostral scale wider than high (vs. loreal as long as high and rostral higher than wide); from *A. maculatus* (Günther, 1858) and *A. pantostictus* Fernandes & Puorto, 1993 species groups in having hemipenes usually with lobular crests and belly scattered with dark brown dots or spots eventually forming continuous stripes (vs. hemipenes lacking lobular crests, with alary spines and lateral projections [*A. pantostictus* group], and belly usually immaculate but, when darkened uniformly pigmented [in *A. francoi* Passos, Fernandes, et al., 2010, *A. serranus* Amaral, 1930 and *A. trihedrurus* Amaral, 1926], never light with dispersed dark marks); from *A. bocki* Werner, 1909, *A. edioi* Silva et al., 2005, *A. natans* Hoogmoed & Prudente, 2003, *A. thalesdelemai* Passos, Fernandes, & Zanella, 2005, and *A. torquatus* Duméril, Bibron, & Duméril, 1854 in having 17 dorsal scale rows, seven supralabials, seven infralabials, two postoculars, belly ground color light covered with regular or irregular dark marks, semicapitate and semicalyculate hemipenis with capitular region similar in length or longer than the hemipenial body and usually lobular symmetry (vs. 15 dorsals and belly mostly cream in *A. edioi*; six supralabials in *A. bocki*; lobular asymmetry and capitulum shorter than hemipenial body in *A. natans*; six supralabials, six infralabials, single postocular and belly uniformly cream in *A. thalesdelemai*; usually eight supralabials, eight infralabials, single postocular, and non-capitate non-calyculate organ in *A. torquatus*).

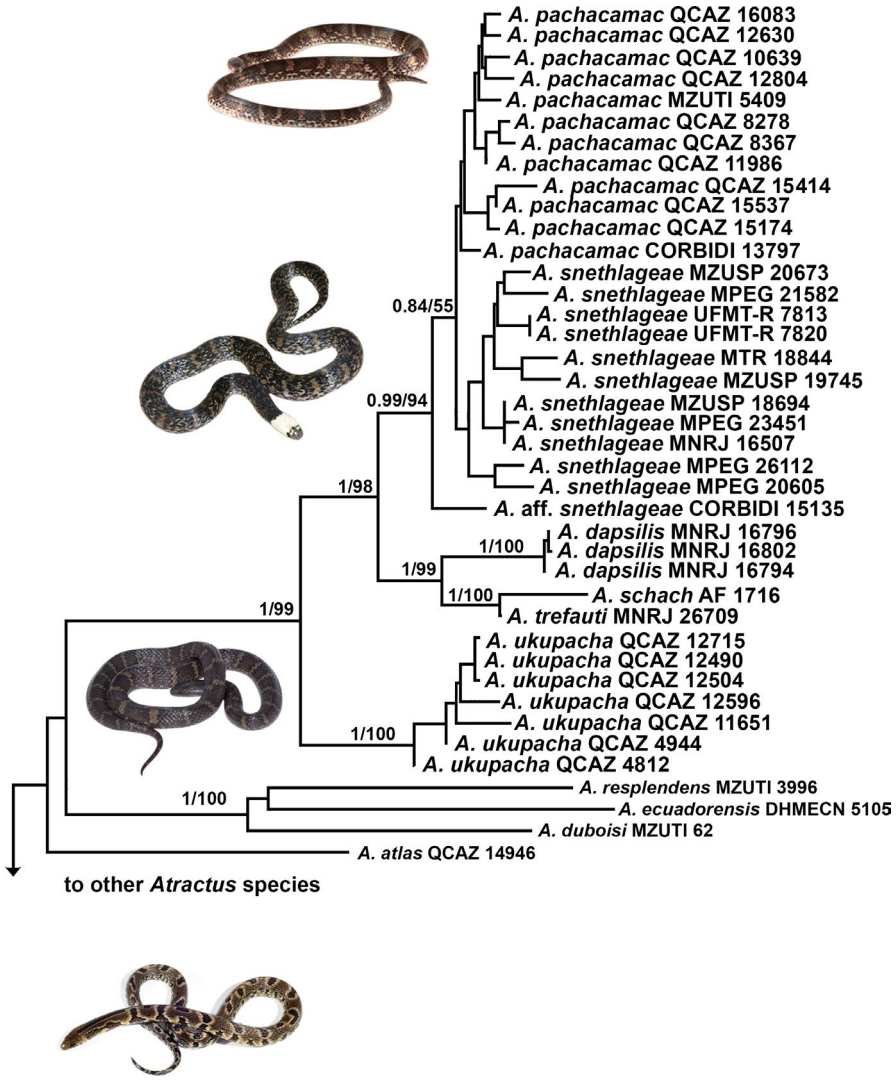

FIGURE 1 Phylogeny of the *Atractus snethlageae* complex. Maximum likelihood tree based on phylogenetic analysis of six genes (*16S*, *CMOS*, *CYTB*, *ND4*, *NT3*, and *RAG1*). Posterior probabilities and Bootstrap values are separated by "/"

3.3 | Species account

Order Squamata Oppel, 1811

Family Dipsadidae, Bonaparte, 1838

Subfamily Dipsadinae, Bonaparte, 1838

Tribe Dipsadini, Bonaparte, 1838

Genus *Atractus* Wagler, 1828

Atractus snethlageae Cunha & Nascimento, 1983.

Atractus badius – specimen "E" Boulenger (1894).

Atractus badius – Cunha and Nascimento (1978).

Atractus flammigerus snethlageae – Cunha and Nascimento (1983), *partim* (MPEG 16382 represents *Atractus trefauti*); Cunha and Nascimento (1993).

Atractus snethlageae – Vanzolini (1986b); Jorge-da-Silva (1993); Doan and Arizabal (2000); Frota (2000); Frota (2004); Giraudo and Scrocchi (2000); Giraudo (2004); Bernarde and Abe (2006); Gutsche et al. (2007); Gonzales and Embert (2008); Passos and Fernandes (2008), *partim*; Prudente and Passos (2008), *partim*; Ávila-Pires et al. (2009); Marçal et al. (2011); Bernarde et al. (2012); Schargel et al. (2013), *partim*; Vaz-Silva et al. (2015), *partim*.

Atractus flammigerus – Dixon and Soini (1986); Duellman and Salas (1991); Jorge-da-Silva (1993); Duellman (2005); Doan and Arizabal (2002); Carrillo de Espinoza and Icochea (1995).

Atractus schach – Nascimento et al. (1988); Passos and Fernandes (2008), *partim*; Prudente and Santos-Costa (2005); Prudente and Passos (2008), *partim*; Bernarde et al. (2011); Bernarde et al. (2012); Waldez et al. (2013); Vaz-Silva et al. (2015), *partim*; Rodrigues et al. (2016); Bernarde et al. (2017).

Atractus sp. – Silva et al. (2012); Melo-Sampaio et al. (2019).

Holotype: MPEG 10131, adult male from Brazil, Pará, Colônia Nova, 10 km near Gurupi river, on the BR-316 highway. The type locality is herein restricted to municipality of Cachoeira do Piriá

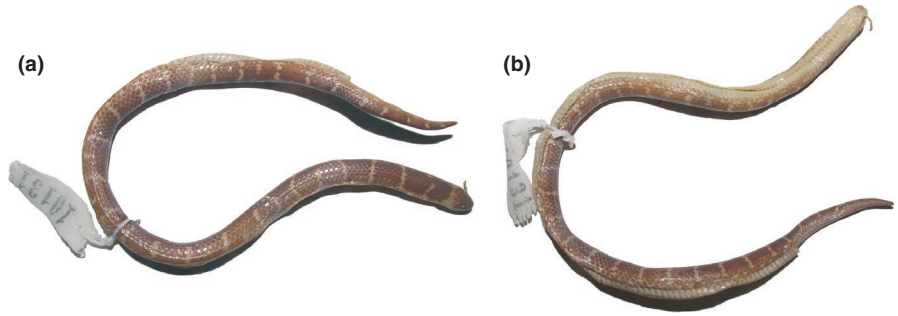

FIGURE 2 Dorsal (a) and ventral (b) views of *Atractus snethlageae*. Holotype (MPEG 10131) from Cachoeira do Piriá, Pará, Brazil

(1.821°S, 46.402°W), 29 m above sea level (hereafter asl), collected by O.R. da Cunha and F.P. do Nascimento on 3 October 1976 (Figure 2; Figure S3).

Paratypes (*n* = 11): All collected by O.R. da Cunha and F.P. do Nascimento in Brazil. Six females: Pará, Ananindeua, Lago Azul (1.383°S, 48.406°W), 33 m asl, MPEG 16383, 16384 (the last incorrectly numbered as MPEG 16387); Capanema, Bela Vista (now Tauari Village), (1.131°S, 47.065°W) 37 m asl; MPEG 2543 (stated as male in original description); Belém, Mosqueiro Island (1.151°S, 48.378°W) 34 m asl, MPEG 2595; Maranhão, Junco do Maranhão, Nova Vida (1.825°S, 46.107°W) 31 m asl, MPEG 14986, 15422. Five males: Pará, Ananindeua, Lago Azul (1.383°S, 48.406°W) 33 m asl, MPEG 16385; Belém, São João da Pratinha (1.368°S, 48.476°W), 20 m asl, MPEG 10137; Capanema, Bela Vista (now Tauari Village), (1.131°S, 47.065°W), 37 m asl, MPEG 6845, 15973; Santa Bárbara do Pará (formerly Benevides) (1.228°S, 48.292°W), 16 m asl, (MPEG 3955) (Figure 3).

Diagnosis: *Atractus snethlageae* can be distinguished from all congeners by the unique combination of the following characters: (1) smooth dorsal scale rows 17/17/17; (2) postoculars two; (3) loreal moderately long; (4) temporal formula 1+2; (5) supralabials usually seven, third and fourth contacting eye; (6) infralabials usually eight, first four contacting chinshields; (7) maxillary teeth six; (8) gular scale rows three; (9) preventrals one to four (usually three); (10) ventrals 147–163 in females, 137–155 in males; (11) subcaudals 21–24 in females, 27–34 in males; (12) in preservative, dorsum pale brown with irregular pale yellowish transversal bands; (13) in preservative, venter usually cream with brown midventral line; (14) body moderately long in females (maximum 400 mm SVL) and males (maximum 310 mm SVL); (15) tail short in females (8.2%–11.3% of SVL) and moderately long in males (13.3%–16% of SVL); and (16) hemipenes slightly to moderately bilobed (≤ half the length of capitulum), semicapitate and semicalyculate.

Comparisons: We compared *Atractus snethlageae* with the remaining allopatric species of the clade: *A. dapsilis*, *A. schach*, and *A. trefauti*. *Atractus snethlageae* differs from *A. dapsilis* by having ≤163 ventrals in females, ventral mean = 145.7 in males, fully everted hemipenes slightly to moderately bilobed, and retracted organs extending to the level of eighth subcaudal (vs. ≥167 ventrals in females, ventral mean = 159.5 in males, fully everted hemipenes strongly bilobed, and retracted organs extending to the level of 10–12th subcaudal); from *A. schach* by having usually six maxillary teeth and hemipenes semicapitate (vs. seven maxillary teeth and hemipenes without capitular groove); from *A. trefauti* by having usually six maxillary teeth, and tail ≥13.3% of SVL in males and dorsal ground color varying from Vandyke brown to Amber in the "light" morph (vs. often seven maxillary teeth, tail ≤13.2% of SVL in males and black dorsum). Among Amazonian sympatric congeners, *A. snethlageae* shares only with *A. badius*, *A. boimirim* Passos et al., 2016, *A. flammigerus*, *A. major* Boulenger, 1894, *A. natans* Hoogmoed & Prudente, 2003, *Atractus tartarus* Passos et al., 2016 and *A. torquatus* usually a blotched or banded color pattern. *Atractus snethlageae* differs from *A. boimirim* and *A. tartarus* by having 17/17/17 dorsal scale rows (vs. 15/15/15 dorsal scale rows); from *A. badius* by having dorsum light covered with dark marks or dark with light marks (vs. dorsum red with conspicuous black dyads separated by white band; see Passos et al. in press); from *A. flammigerus* by having usually seven supralabials and lacking keels on the dorsal scales (vs. eight supralabials and keels covering dorsal scale rows); from *A. major* by having usually four infralabials contacting chinshields and seven maxillary teeth (vs. three infralabials contacting chinshields and six maxillary teeth); from *A. natans* by having ventral surface of body mostly creamish white covered by few dark brown blotches usually linearly arranged on the midventer (vs. belly almost entirely black except for the lateral sides of ventral scales creamish white); from *A. torquatus* by having two postoculars and seven supralabials (vs. usually one postocular and eight supralabials; see Passos & Prudente, 2012). We refer to Table 1 for additional comparisons between *Atractus snethlageae* and other Amazonian congeners.

Description of the holotype: We refer to Cunha and Nascimento (1983) and describe additional features. SVL 182 mm, TL 30 mm; midbody diameter 5.3 mm. Rounded head in lateral view; symphysial three times wider than high; gular scale rows three; preventrals four; loreal moderate touching second and third supralabials; nasal divided; internasals reduced, slightly wider than long; rostral not visible from above, about twice as wide as high; prefrontals longer than wide, fused posteriorly; supraocular small, squared, shorter than eye diameter; frontal triangular as long as wide; parietals twice as long as wide; postoculars 2/2; temporals 1+2, posterior ones larger; pupil rounded; supralabials seven, with first shorter and narrower than second; second and third supralabials in contact with loreal;

FIGURE 3 Color pattern variation of *Atractus snethlageae*. Paratypes: MPEG 3955 (a), MPEG 15973 (b), MPEG 6845 (c), MPEG 16383 (d), MPEG 2595 (e), and MPEG 10137 (f)

infralabials eight, first four (right) and first five (left) touching chinshields; ventrals 137; subcaudals 29; maxillary teeth six.

Color in preservative: Dorsum of head olive-brown [color 278] including posterior portion of parietals; nuchal band Straw Yellow [color 53] (two and a half scales long), reaching occipital region, except for the first dorsal scale row; ventral portion of supralabials cream [color 12]; infralabials and gular region cream [color 12]; symphysial, first two pair of infralabials and first third of chinshields stained with sepia dots; body dorsum Vandyke brown [color 38] with third row beige [color 254], light yellow ocher [color 13] bands one-half to one scale long connected or not on the vertebral axis; venter cream with an irregular midventral sepia stripe [color 279], increasing in width gradually on posterior portion of body; tail ventrally Raw siena [color 32] (Figure 2).

Color in life: The extreme dark morph is represented by MZUSP 21474, with sepia dorsum of head covering frontal and postoculars, and a pale buff [color 1] band covering temporals, parietals, one row of occipitals, and two last supralabials; sepia body dorsum with buff transverse bands one-half to one scale long interrupted or not on the vertebral axis; venter light buff with Burnt umber spots forming midventral line; venter of specimen UFRO-H 2549 immaculate chamois [color 83] on the first quarter, with tiny sepia dots increasing in number posterior to midbody, forming a diffuse midventral line at the level of six scales before cloaca (Figure 3).

Color variation in preservative (n = 128): Dorsum of head with olive-brown [color 278] cephalic-cap, extending from rostral to medial region of parietal; posterior portion of parietal and temporal region ground cinnamon [color 270], constituting an occipital band of variable size, but variable in width and length; occipital band ground cinnamon with medial constriction or trapezoidal-shaped, being posteriorly limited by background color of body; occipital band eventually wider, extending dorsally over posterior region of parietal until first dorsal with cinnamon pigmented; occipital band occasionally indistinct, making head entirely sepia dorsal and laterally; head laterally sepia [color 279] to anterior region of sixth supralabial and predominantly cream after postorbital region; temporal and occipital regions generally creamy, with irregular brown spots invading anterior portion of temporals; temporal and occipital regions become uniformly cream with enlargement of occipital band; supralabial usually brown to the level of sixth

TABLE 1 Selected features for comparisons among *Atractus* species closely related to or previously associated (in literature or scientific collections) with *Atractus snethlageae* species complex.

	VE		SC						
SPECIES	F	M	F	M	SL	IL(CH)	MT	LPB	Dorsal coloration
A. akerios	149–156	140–145	19–20	27–33	7	8 (4)	6	Absent	Antique brown with russet spots
A. atlas	158–169	NA	28–33	NA	8	8 (4)	8	Absent	Yellow ocher with black bands
A. dapsilis	167–182	152–166	21–26	30–37	7	8 (4)	6–7	Absent	Tawny oliver with raw umber bands / Grayish brown with cinnamon bands
A. major	154–181	149–170	27–37	31–45	7	7(3)	6–7	Absent	Cinnamon drab with cinnamon brown bands/ Fawn color with warm sepia bands
A. nawa	166–169	NA	16–20	NA	7	7 (4)	7	Absent	Brussels brown with Raw umber spots
A. pachacamac	162–175	158–167	31–33	39–45	7	8 (4)	7	Absent	Sepia with saval brown bands
A. schach	148–150	142–151	19–21	25–32	7	8 (4)	7	Absent	Olive brown with black regular bands
A. snethlageae	147–163	137–155	21–24	27–34	7	8 (4)	6	small/ incomplete	Vandyke brown with light yellow ocher bands
A. touzeti	167–170	NA	31	NA	8	7 or 8 (4)	8	Absent	Short pale crossbands Edged by black borders
A. trefauti	153–158	139–149	21–24	24–29	7	8 (4)	5–7	Incomplete	Black with beige bands
A. ukupacha	161–170	154–165	23–29	38–42	7	8 (4)	7	Absent	Dusky brown with olive-brown bands

Abbreviations: IL(CH), Infralabials (in contact with chinshields); LPB, light parietal band; MT, maxillary teeth; SC, subcaudals; SL, supralabials; VE, ventrals. The SL, IL(CH), MT, and LPB were placed together for both sexes because these variables are not secondarily dimorphic. NA, not available.

scale and predominantly cream on the remained supralabials; supralabial occasionally entirely sepia; gular region cream with black spots on the symphysial, first pair of infralabials, mesial region of infralabials and anterior portion of chinshields; preventrals usually uniformly cream; gular region eventually densely stained by irregular brown dots; belly with background color varying from uniform ground cinnamon to predominantly grayish horn [color 268], usually with round hair brown spots located on the middle of each ventral scales forming conspicuous (but frequently discontinuous) midlines throughout body; spots occasionally laterally expanded, constituting enlarged ventral bands or concentrating on anterior part of ventral scales; belly occasionally thickly stained with brown scoring, more concentrated on the middle and posterior third of body; tail usually hair brown uniform or irregularly invaded by ground cinnamon spots; body dorsally sepia with 24–34 transverse bands; bands brownish olive or yellowish cream (one to two scales in length) alternated on the flanks and, occasionally connected to opposite one on the vertebral region forming narrow rings separated by sepia interspaces (four to seven scales long); bands generally extending into paraventral region; possibly with an irregular pattern, with diffuse and longitudinally oriented spots (Figure 4). For the specimens with "light" morphotype the colors varying from dorsum Amber (MZUSP 21464) to Cinnamon Drab with fuscous bands (UFRO-H 2548), connected on the vertebral axis, two or three scales long. Parietal band is often cream white (also cinnamon drab to cinnamon brown).

Hemipenial morphology (n = 6): Organs in situ (retracted) extend to the level of eighth subcaudal and bifurcate at the level of seventh subcaudal (n = 2). Fully everted and maximally expanded hemipenes renders a slightly (more frequently, ≤ half capitulum length) to moderately (more rarely, ≥ half capitulum length) bilobed, semicapitate and semicalyculate organ; lobular region wider than hemipenial body; lobes centrolinearly oriented and flattened, clavated or attenuated (rarely) on the tip; lobes with lateromesial expansion toward intrasulcar region (Figure 5b–f), sometimes only evident nearly to lobe bifurcation (Figure 5e); lobes symmetrical and presenting proximal portion from intrasulcar region with straight base; straight base more conspicuous in conical or attenuate organs (Figure 5); lobes uniformly covered with spinulate calyces on both sides of hemipenes; spinules usually replaced by irregular papillae toward apices of lobes; capitular groove usually distinct on both faces of organ; capitular groove generally indistinct in slightly bilobed hemipenes and more conspicuous in moderately bilobed organs (Figure 5); capitulum with transversal spinulated flounces formed by union of horizontal walls of calyces; calyces lacking vertical walls along the sulcate and asulcate faces of capitulum; conspicuous transversal calyculated flounces with irregular rows on the intrasulcar region; hemipenial body elliptical covered with enlarged hooked spines; larger spines generally located laterally below sulcus spermaticus bifurcation; distal region of hemipenial body on maximally expanded organ with rows of spines concentrating in the middle of asulcate face; sulcus spermaticus bifurcates approximately on the 50% of organ length; sulcus spermaticus margins relatively thick at level of division and along the capitular region; sulcus spermaticus not bordered by spinules;

FIGURE 4 Color in life of *Atractus snethlageae*. Uncatalogued specimen from Porto Velho, Rondônia, Brazil (a, b). MPEG 20362 from Nova Mamoré, Rondônia, Brazil (c). MTR 18844 from Beruri, Amazonas, Brazil (d). Itaituba, Pará, Brazil (e). Cruzeiro do Sul, Acre, Brazil (f). Photos by D. Meneghelli (a), U. Oliveira (b), L. Vitt (c), M. Teixeira Jr. (d), L. Moraes (e), S. Albuquerque (f)

basal naked pocket restricted to most basal region of hemipenial body; proximal region of hemipenes body covered with few hooked spines and dispersed spinules (Figure 5).

Quantitative variation (*n* = 128): Largest female 420 mm SVL, 40 mm TL; largest male 335 mm SVL, 55 mm TL; ventrals 147–163 (mean = 155.1; *n* = 61; SD = 5.3) in females, 137–158 (mean = 145.7; *n* = 54; SD = 7.9) in males; subcaudals 17–26 (mean = 22.9; *n* = 61; SD = 0.9) in females, 26–39 (mean = 31.4; *n* = 54; SD = 2.5) in males; supralabials seven (*n* = 27 sides) or eight (*n* = 7 sides); infralabials seven (*n* = 2 sides), eight (*n* = 31 sides) or nine (*n* = 1 side); preventrals one (*n* = 4), two (*n* = 10), three (*n* = 88) or four (*n* = 11); maxillary teeth five (*n* = 2 sides), six (*n* = 52 sides), seven (*n* = 144 sides) or eight (*n* = 10 sides).

Distribution: *Atractus snethlageae* occurs in southern Amazonia (from Maranhão state in Brazil to Peru), with a few records in northern Amazonia (on the north side of the Amazon River) only in the western portion of Amazonia (Amazonas state in Brazil, Colombia, Peru, and Ecuador) (Figure 6).

Remarks: Cunha and Nascimento (1978) first identified *A. snethlageae* as *Atractus badius*. However, the corresponding specimen was not included within the type series of *A. flammigerus snethlageae* (Cunha & Nascimento, 1983). When examining the type series, we found that there is a typographical error in relation to female paratype MPEG 16387, which is MPEG 16384. Moreover, we were not able to find the "tubercles" mentioned by Cunha and Nascimento (1983), since the dorsal scales are entirely smooth. Hoogmoed and Prudente (2003) have hypothesized that anomalous conditions of internasal scales in prefrontal suture should be evaluated regarding relationship among *Atractus*. *Atractus snethlageae* was described based on a series of 13 specimens from the states of Amapá, Maranhão, and Pará, Brazil. However, specimen MPEG 16382 from Serra do Navio was recently recognized as *A. trefauti*, making the original type series of *A. snethlageae* composite (Melo-Sampaio et al., 2019). The central Amazonian records of *A. snethlageae* in the Manaus region by Fraga et al. (2013) belong to a dark morph of *A. dapsilis*. The Argentinian record of *A. snethlageae* (Giraudo & Scrocchi, 2000) is tentatively maintained as *A.* cf. *snethlageae* due to the presence of a conspicuous light parietal band (see Giraudo, 2004). On the other hand, the Ecuadorian populations assigned to *A. snethlageae* by Schargel et al. (2013) are recognized herein as two separate species (see below).

Atractus ***nawa*** **sp. nov.**

urn:lsid:zoobank.org:act:E96A9F8B-8D29-4A9F-A13B-650DAE22DCAC

Atractus major – Ávila-Pires et al. (2009).

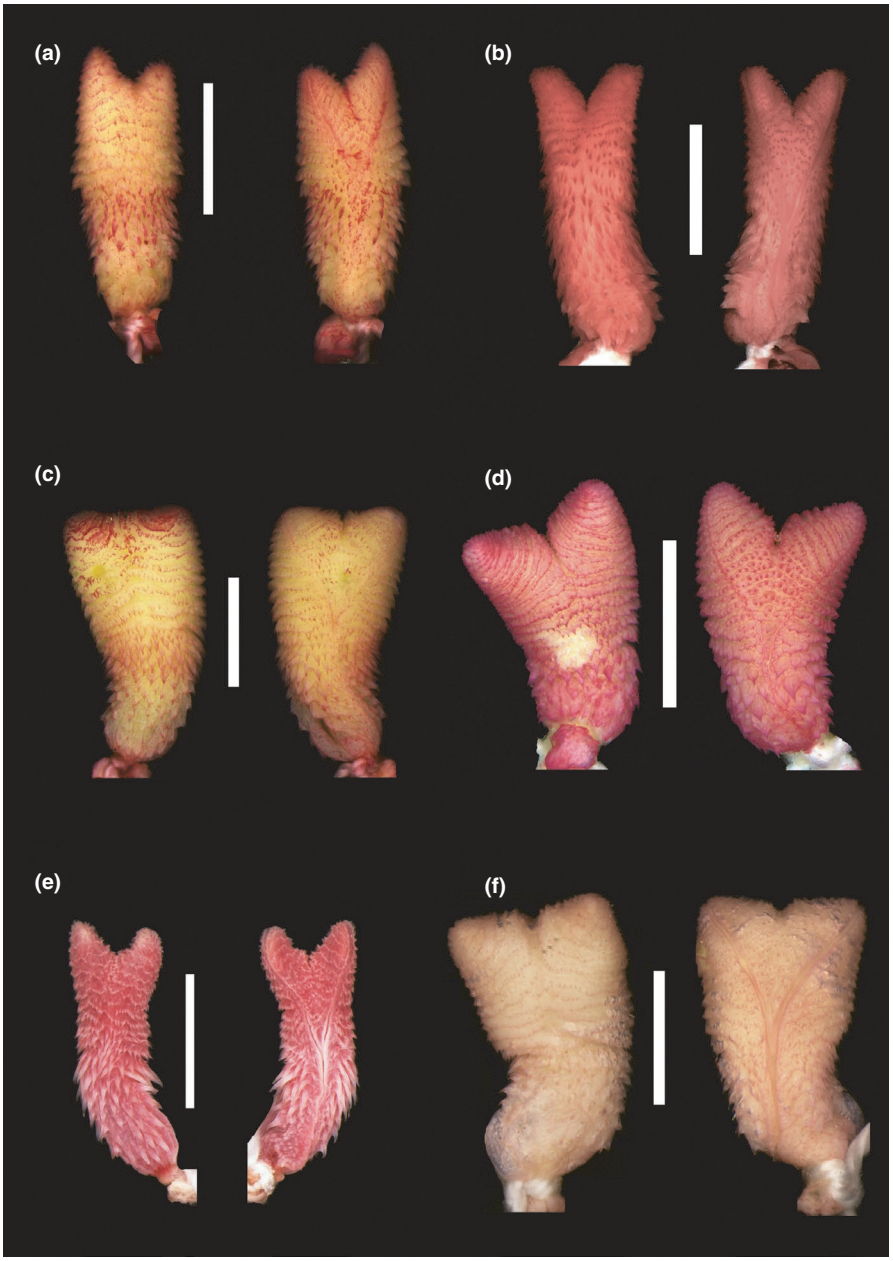

FIGURE 5 Hemipenial morphology of *Atractus snethlageae*. Asulcate (left) and sulcate (right) views of the organs of specimens from Colniza, Mato Grosso, Brazil (UFMT-R 7813 - a); Itaituba, Pará, Brazil (MPEG 24564 - b); Machadinho d'Oeste, Rondônia, Brazil (MZUSP 21982 - c); Anamã, Amazonas, Brazil (INPA-H 9524 - d); Porto Velho, Rondônia (MPEG 17877 - e); and Belém, Pará, Brazil (MPEG 10137, paratype - f). Scale bar = 5 mm

Atractus schach – Passos and Fernandes (2008), *partim*; Prudente and Passos (2008), *partim*.

Holotype: MPEG 20376 (field number LJV 6299), adult female from Brazil, Acre, Porto Walter (8.258°S, 72.776°W), 212 m asl, collected by L.J. Vitt, T.C.S. Avila-Pires, J.P. Caldwell, and V. Oliveira on 28 February 1996 (Figure 7).

Paratype: UFACF 3771, adult female from Brazil, Acre, Cruzeiro do Sul, km 80 of the BR-364 highway on the route to Tarauacá (7.750°S, 72.366°W), 200 m asl, collected by R.A. Machado on February 2010.

Etymology: The specific epithet "nawa" corresponds to the self-designation or to an indicator of otherness (other people) of many Pano-speaking societies living along Juruá River basin (Montagner, 2007). The word also refers to the distinction of the new species from its congeners by indigenous people on the region.

Diagnosis: *Atractus nawa* can be distinguished from all congeners by unique combination of the following characters: (1) smooth dorsal scale rows 17/17/17; (2) postoculars two; (3) loreal moderately long; (4) temporal formula 1+2; (5) supralabials seven, third and fourth contacting eye; (6) infralabials seven, first four contacting chinshields; (7) maxillary teeth seven; (8) gular scale rows four; (9) preventrals four; (10) ventrals 166–169 in females, unknown in males; (11) subcaudals 16–20 in females, unknown

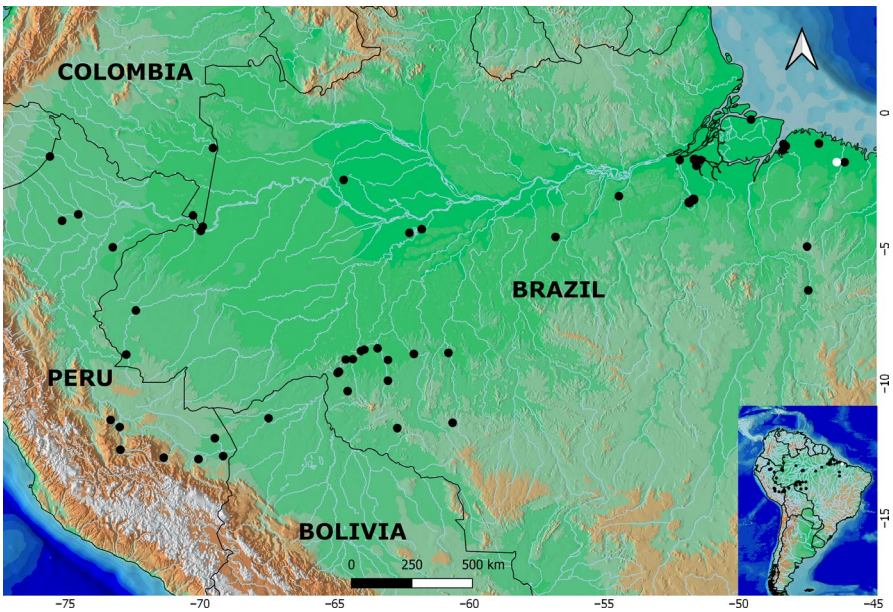

FIGURE 6 Known distribution of *Atractus snethlageae*. Type locality is represented by white dot

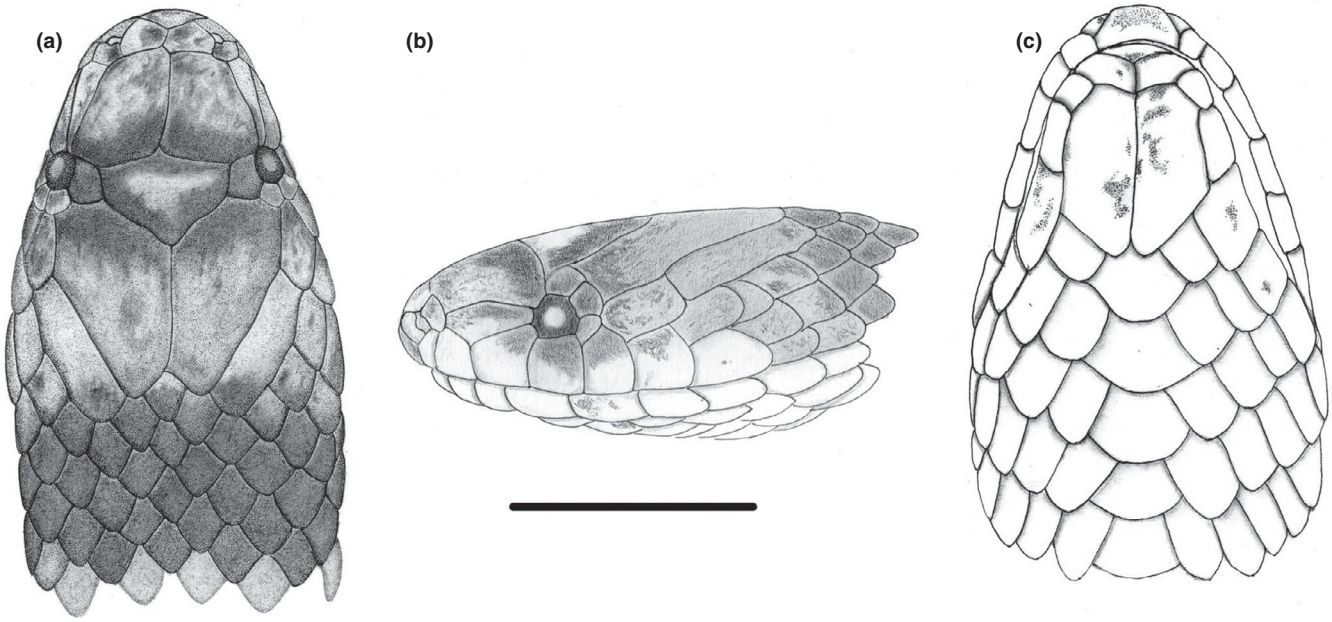

FIGURE 7 Dorsal (a), lateral (b), and ventral (c) views of *Atractus nawa*. Holotype (MPEG 20376) from the municipality of Porto Walter, state of Acre, Brazil. Scale bar 5 mm

in males; (12) in preservative, dorsum Brussels brown [color 33] with Raw umber spots; (13) in preservative, venter predominantly pale cinnamon with warm sepia dots near cloaca and midventral portion of tail; (14) body size moderately long in females (maximum 405 mm SVL); and (15) tail short in females (6.2–7.7% of SVL); (16) hemipenis unknown.

Comparisons: We compared the new species with geographically closer and sympatric congeners occurring along the state of Acre, Brazil. *Atractus nawa* differs from *A. albuquerquei*, *A. boimirim*, *A. emmeli*, and *A. elaps* by having 17/17/17 dorsal scale rows (vs. 15/15/15). Regarding the species with 17 dorsal scales rows, *A. nawa* differs from *A. major* in having first four infralabials in contact with chinshields, dorsal Brussels brown with Raw umber spots, pale cinnamon with warm sepia dots near cloaca, and ≤20 subcaudals in females (vs. first three infralabials in contact with chinshields, dorsum gray or reddish, followed by square sepia dots from midbody to posterior region of belly and >27 subcaudals in females); from *A. snethlageae* in having tail <8% of SVL in females, ≤20 subcaudals in

females, ≥166 ventrals in females, and pale orange snout (vs. tail >8% of SVL in females, >26 subcaudals in females, ≤163 ventrals, and olive brown snout); from *A. latifrons* in having loreal scales twice as long as high and rostral scale wider than high (vs. loreal as long as high and rostral higher than long). We refer to Table 1 for additional comparisons between *Atractus nawa* and other Amazonian congeners.

Description of the holotype: SVL 390 mm, tail length 30 mm (7.7% of SVL); head slightly distinct from body; head length 11.1 mm (3% of SVL); head width 7.0 mm (63.1% head length); rostral–orbit distance 3.9 mm; nostril–orbit distance 2.8 mm; interorbital distance 4.1 mm; head rounded in lateral view; snout truncate in dorsal view, truncate in lateral view; canthus rostralis conspicuous; rostral subtriangular in frontal view, 2.0 mm wide, 1.2 mm high, well visible in dorsal view; internasal 0.9 mm long, 1.1 mm wide; internasal suture sinistral with respect to prefrontal suture; prefrontal 2.7 mm long, 2.6 mm wide; supraocular subtrapezoidal, 1.1 mm long, 1.1 mm wide at broadest point; frontal bell-shaped, 2.5 mm long, 3.7 mm wide; parietal 5.0 mm long, 3.0 mm wide; nasal entirely divided, nostril divided in both parts; prenasal 1.0 mm high, 0.5 mm long; postnasal 1.0 mm high, 0.9 mm long; loreal 2.2 mm long, 1.0 mm high; second and third supralabials contacting loreal; third and fourth supralabials entering the orbit; eye diameter 1.2 mm; pupil rounded; two postoculars similar in height, being lower shorter than upper; upper postocular 0.7 mm long, 0.8 mm high; lower postocular 0.6 long, 0.7 mm high; temporal formula 1+2; first temporal 2.0 mm long, 1.4 mm high; upper posterior temporals 3.8 mm long, 1.2 mm wide; supralabials seven, third and fourth contacting eye; first supralabial shorter (0.8 mm high) than second (1.1 mm high) and smaller in length (0.7 mm) than second (1.0 mm); third supralabial pentagonal, larger in height (1.4 mm) and longer (1.4 mm) than second; sixth supralabial taller than third (1.7 mm); seventh longer than third (2.5 mm) supralabial; symphysial triangular, 1.8 mm wide, 0.5 mm long; first pair of infralabial preventing symphysial–chinshields; infralabials seven, first four contacting chinshields; chinshields 3.5 mm long, 1.7 mm wide; gular scale rows four; preventrals four; ventrals 169; subcaudals 18 respectively from left to right side; dorsal scale rows 17/17/17, lacking apical pits and supracloacal tubercles; midbody diameter 10.1 mm (2.6% of SVL); caudal spine 1.1 mm long, smaller than last subcaudal scale (1.3 mm); anal single. Maxillary bone arched upward anteriorly in lateral view, ventral portion curved on anterior and nearly flattened on median to posterior portion; maxillary with seven teeth; teeth angular in cross section, robust at base, narrower at apices, slightly curved posteriorly; teeth similar in size and spacing; last teeth slightly smaller and in same spacing to anterior ones; maxillary "diastema" absent; lateral process of maxilla well developed.

Dorsum of head Brussels brown with interocular stripe Raw umber and center of frontal extending into subocular region; snout with a small Raw umber spot between internasals and posterior part of rostral; supralabials and infralabials trogon yellow [color 81] to light orange yellow [color 77]; dorsal scales flesh ocher splecked [color 57] on dorsum of body Brussels brown with

FIGURE 8 General view of the holotype of *Atractus nawa* (MPEG 20376) in life from Porto Walter, state of Acre, Brazil. Photo by L. Vitt

Raw umber spots rectangular (four scales wide and two scales long), bordered with cream spots; nuchal band Raw umber with five scales long; paraventral line extending along the body at the level of second dorsal scale row; venter predominantly pale cinnamon with warm sepia dots near cloaca and midventral portion of tail (Figure 8).

Color in life (*n* = 2): Dorsum of head black with snout and parietals orange, followed by black parietal band and black spots bordered by yellowish pigment; belly well-distinct reddish-pink, limited by narrow black paraventral lines. Iris brown with rounded black pupil (Figure 9). The paratype agrees well with the holotype in dorsal color pattern. Some differences are found in the extension of Raw umber bands being inconspicuous light-bordered.

Quantitative variation (*n* = 2): Largest female 390 mm SVL, 30 mm TL; ventrals 166–169 (mean = 167.5; *n* = 2; SD = 2.1) in females; subcaudals 18–20 (mean = 19; *n* = 2; SD = 1.4) in females; adult midbody diameter 9.2–10.1 mm in females; maxillary teeth six (*n* = 2 sides) or seven (*n* = 2 sides).

Distribution: This species is only known from two localities in upper Juruá river basin, state of Acre, Brazil (Figure 10).

Remarks: The type locality where *A. nawa* was collected in Porto Walter has been deforested for cattle pasture (Vitt et al., 1997; P.R. Melo-Sampaio, pers. obs.). The site where paratype was collected is also suffering with deforestation along BR-364 highway.

Atractus ***pachacamac*** **sp. nov.**

urn:lsid:zoobank.org:act:BE85090A-B08C-4AA5-8EAD-3211ED8396C7

Atractus snethlageae – Schargel et al. (2013), *partim*; Yánez-Muñoz & Venegas (2008); Camper and Zart (2014).

Atractus touzeti – Arteaga et al. (2017).

Atractus aff. *snethlageae* – von May and Mueses-Cisneros (2010).

Atractus cf. *snethlageae* – Rodríguez and Knell (2004).

Atractus major – Duellman (1978).

Holotype: QCAZ 12630, adult male from Ecuador, Napo, Sumaco Wildlife Sanctuary, Sendero Benavides (0.676°S, 77.600°W), 1496 m asl, collected by F. Ayala on 4 April 2014.

Paratopotypes (*n* = 4): QCAZ 11986, 12804, adult females, collected by J. Camper on 23 July 2014; QCAZ 10639, adult male

FIGURE 9 Color in life of *Atractus nawa*. Uncollected specimen from Santa Luzia Village, Cruzeiro do Sul, Brazil (a–d). Note the light orange snout. Photos by D. Paiva

FIGURE 10 Known distribution of *Atractus nawa*. Type locality is represented by white dot

collected by J. Camper on 11 July 2010; QCAZ 16083, adult male same data as holotype.

Paratypes (*n* = 24): Ecuador: Morona Santiago: General Proaño, Central Hidroeléctrica Abanico (2.245°S, 78.195°W), 1600 m asl, EPN 11454 and EPN 11455, adult females collected by Y. Sagredo on 29 March 2007; Cotundo, at km 32 from the road Cocodrilos-Tena (0.681°S, 77.800°W), 1476 m asl, QCAZ 11075, adult female collected by F. Velásquez on 28 November 2010; Taisha, Makuma, Paatim Shuar Center (2.133°S, 77.650°W), 715 m asl, FHGO 10080, adult male collected by native people on 16 April 2014. Napo: Gonzalo Pizzaro, El Reventador (0.016°N, 77.377°W), 1720 m asl, DHMECN 11556, adult female collected

by M. Yánez-Muñoz and team between 11–14 December 2014; El Chaco, Sardinas (0.340°S, 77.810°W) 1300 m asl, QCAZ 1493, adult male collected by G. Onore on 18 October 1986; Chontapunta, Sumac Sacha (0.965°S, 77.314°W), 350 m asl, FHGO 2178, adult male collected by F. Salazar, E. Salinas, R. Duque and I. Velasco on 16 June 1998. Orellana: Dayuma, Pozo Petrolero Capirón (0.665°S, 76.468°W), 240 m asl, EPN 7358, adult female collected by A. Almendáriz on 17 March 2000; Joya de los Sachas, San Sebastian del Coca (0.142°S, 76.992°W), 350 m asl, EPN 11701, adult female collected by A. Almendáriz on 6 May 2002; Nuevo Paraíso, Village Juan Pablo II (0.302°S, 77.179°W), 291 m asl, EPN 5471, adult male collected by A. Almendáriz on 12 April 1996; Aguarico (0.792°S, 75.901°W), 217 m asl, EPN 10548, adult male collected by A. Almendáriz and F. Grefa on 23 March 2006; Yasuní National Park (0.492°S, 76.557°W) 252 m asl, QCAZ 10614, adult male collected by M. Read on 29 January 1996. Pastaza: Tzarentza (1.356°S, 78.058°W), 1355 m asl, MZUTI 5409, collected by J. Vieira on 10 May 2016; Villano, Kurintza (1.507°S, 77.511°W), 362 m asl, QCAZ 8278, juvenile collected at by D. Paucar on 29 July 2008; Villano, K10 camp (1.476°S, 77.534°W), 475 m asl, QCAZ 8367, adult female collected by E. Carrillo on 11 October 2008 and QCAZ 11833, adult male collected by J. Brito on 1 October 2013. Sucumbíos: Lago Agrio, El Eno (0.064°S, 76.879°W), 278 m asl, FHGO 5813, adult male collected by M. Alcoser. Zamora-Chinchipe: Yanzatza, Los Encuentros (3.765°S, 78.502°W; 1450 m asl), QCAZ 15174, adult female collected by D. Chávez on 18 November 2016, and MECN 8437 adult female collected by P. Galvis on November 2017; Reserva Natural Maycu (4.248°S, 78.658°W), 879 m asl, QCAZ 15414, adult female collected by D. Almeida on 28 February 2017; El Zarza (3.776°S, 78.497°W), 1450 m asl, adult female QCAZ 15537, collected by P. Baldeón on 2 March 2017; El Pangui, Concesión Minera Princesa (3.896°S, 78.516°W), 1587 m asl, MECN 13078, adult male collected by D. B. Zapata on 24 January 2016. Peru: Loreto: Datem del Marañon, Cahuapana (5.664°S, 76.839°W), 1150 m asl, CORBIDI 13797 adult male collected by P. J. Venegas on October 2014; Maynas, Güeppi (0.018°S, 75.358°W), 220 m asl, CORBIDI 167, adult male collected by P. J. Venegas and M. Yanez-Muñoz on 22 October 2007.

Etymology: According to the Inca mythology, Pachacámac or Pacha Kamaq ("creator of the land"; being pacha: "land" and kamaq: "creator" or "created" in Quechua language) was a god. The Pachacámac, son of the sun, came to our world and climbed to the highest summit (perhaps a volcano) to throw four stones to the four cardinal points, thereby taking possession of everything that covered his sight and reached his stones. The name also refers to fossorial lifestyle in high elevations.

Diagnosis: *Atractus pachacamac* can be distinguished from all congeners by unique combination of the following characters: (1) smooth dorsal scale rows 17/17/17; (2) postoculars two; (3) loreal moderately long; (4) temporal formula 1+2; (5) supralabials seven, third and fourth contacting eye; (6) infralabials usually eight, first four contacting chinshields; (7) maxillary teeth seven; (8) gular scale rows three; (9) usually two preventrals; (10) ventrals 162–175 in females, 158–167 in males; (11) subcaudals 31–33 in females, 39–45 in males; (12) in preservative, dorsum sepia with saval brown bands; (13) in preservative, venter chamois anteriorly and sepia with chamois spots posteriorly; (14) long body in females (maximum 620 mm SVL) and moderately long in males (maximum 460 mm SVL); (15) tail size moderately long in females (12.1–13.6% of SVL) and long in males (17.5%–19.5% of SVL); and (16) hemipenes moderately bilobed (≤half the length of capitulum), semicapitate, and semicalyculate.

Comparisons: *Atractus pachacamac* differs from *A. snethlageae* in having ≥158 ventrals, ≥39 subcaudals, and >320 mm SVL in males (vs. ≤155 ventrals, ≤34 subcaudals and <300 mm SVL in males); from *A. nawa* in having >30 subcaudals, tail >12.0% SVL, and >600 mm SVL in females, (vs. ≤20 subcaudals, tail ≤8.0% of SVL, and ≤405 mm SVL in females); from *A. dapsilis* in having >600 mm SVL, tail >12.0% of SVL in females, ≥17.5% of SVL in males, and 31–33 subcaudals in females, 39–45 in males (vs. <600 mm SVL, and <12.0% of SVL in females, ≤17.6% of SVL in males, and 21–26 subcaudals in females, 30–37 in males); from *A. ukupacha* in having >600 mm SVL in females and moderately bilobed hemipenes (vs. spotted preventrals, <500 mm SVL in females, and strongly bilobed hemipenes); from *A. schach* and *A. trefauti* in having >600 mm SVL, tail >12.0% of SVL in females, >17% of SVL in males, 162–175 ventrals in females, 158–167 in males, and 31–33 subcaudals in females, 39–45 in males (vs. <230 mm SVL, tail <12.0% of SVL in *A. schach* and *A. trefauti*; 148–150 ventrals in females, 142–151 in males, 19–21 subcaudals in females, 25–31 in males of *A. schach*; and 153–158 ventrals in females, 139–149 in males, 21–24 subcaudals in females, 24–29 in males of *A. trefauti*); from *A. touzeti* in having <700 mm SVL in females, seven supralabials, third and fourth supralabial contacting eye, seven maxillary teeth, postocular equal in size, and upper and lower posterior temporals equal in size (vs. >700 mm SVL in females, eight supralabials, fourth and fifth supralabial contacting eye, eight maxillary, very small lower postocular, and very large upper posterior temporal). We refer to Table 1 for additional comparisons between *Atractus pachacamac* and other Amazonian congeners.

Description of the holotype: SVL 385 mm, tail length 72 mm (18.7% of SVL); head slightly distinct from body; head length 15.1 mm (3.9% of SVL); head width 8.15 mm (2.1% of head length); rostral-orbit distance 5.53 mm; nostril-orbit distance 3.92 mm; interorbital distance 5.75 mm; head rounded in lateral view; snout rounded in dorsal view, truncate in lateral view; canthus rostralis barely conspicuous; rostral subtriangular in frontal view, 2.42 mm wide, 1.63 mm high, slightly visible in dorsal view; internasal 1.28 mm long, 1.39 mm wide; internasal suture sinistral with respect to prefrontal suture; prefrontal 3.77 mm long, 2.93 mm wide; supraocular subtrapezoidal, 1.98 mm long, 1.56 mm wide at broadest point; frontal bell-shaped, 3.89 mm long, 4.34 mm wide; parietal 6.51 mm long, 3.28 mm wide; nasal partially divided, nostril located mostly in prenasal; prenasal 1.56 mm high, 1.06 mm long; postnasal 1.41 mm high, 0.94 mm long; loreal 3.15 mm long, 1.0 mm high; eye diameter 1.67 mm; pupil rounded; two postoculars similar in shape and size;

upper postocular 1 mm long, 1 mm high; lower postocular 0.66 mm long, 0.95 mm high; temporal formula 1+2; first temporal 2.61 mm long, 1.47 mm high; upper posterior temporal 4.64 mm long, 1.1 mm wide; supralabials seven, second and third contacting loreal, third and fourth contacting eye; first supralabial smaller (1.15 mm high x 0.93 mm long) than second (1.55 mm x 1.0 mm); third supralabial pentagonal, higher (1.82 mm) and longer (2.45 mm) than adjacent supralabials; sixth supralabial as tall as third; seventh longer than third (3.82 mm) supralabial; symphysial subtriangular, 2.10 mm wide, 0.60 mm long; first pair of infralabials preventing symphysial–chinshields contact; infralabials eight, first four contacting chinshields; chinshields 4.90 mm long, 2.12 mm wide; gular scale rows three; preventrals 3; ventrals 160; subcaudals 42/42 on left and right sides, respectively; dorsal scale rows 17/17/17, lacking apical pits and supracloacal tubercles; midbody diameter 9.95 mm (2.6% of SVL); caudal spine 1.32 mm long, larger than last subcaudal scale (0.89 mm); anal single.

Retracted hemipenes extend to the level of 12th subcaudal, bifurcating at 10th subcaudal. Maxillary bone arched upward anteriorly in lateral view, ventral portion curved on anterior and nearly flattened on median to posterior portion; maxillary with seven teeth; teeth angular in cross section, robust at base, narrower at apices, slightly curved posteriorly; teeth similar in size and spacing; last teeth slightly smaller and in same spacing to anterior ones; maxillary diastema absent or indistinct from interspaces; lateral process of maxilla well developed.

Dorsum of head cinnamon brown [color 43] through its extension, covering parietals and two rows of occipital scales; lateral sides of head mikado brown; upper portion of supralabials chamois [color 84] giving a "moustache" pattern; sixth supralabial with a fuscous spot; postocular and anterior temporal; gular region chamois, infralabials and symphysial region with cinnamon brown spots two last infralabials almost completely chamois; first ventral with a cinnamon brown spot followed by seven immaculate chamois ventrals; eighth ventral with cinnamon brown rectangular spot; ninth to fourteenth ventrals immaculate chamois; venter chamois with few dispersed sepia dots until midbody; posterior region of ventral scales sepia pigmented with chamois spots; ventral surface of tail sepia with scattered chamois spots; dorsal ground color sepia [color 279] with conspicuous sayal brown bands (29), one-half to two scale rows wide; interspaces between sayal brown [color 41] bands three to five scales long; first dorsal scale row with chamois and sepia "chess pattern"; dorsal surface of tail sepia with seven conspicuous bands; tip of tail sayal brown.

Color in life of holotype: Rostral, symphisial, and first pair of infralabials almost completely dark brownish olive [color 127]; snout with tiny chrome orange [color 74] dots; iris rounded and brown; cephalic-cap brownish olive [color 276]; dorsum sepia [color 279] with true cinnamon [color 260] to raw umber [color 26] bands (Figure 11).

Color in life variation (n = 4): Dorsum jet black [color 300] with salmon [color 251] and white parietal band; venter white suffused with fuscous [color 283] forming a double stripe in juvenile QCAZ 8278 (Figures 11 and 12).

Color in preservative variation (n = 27): The paratypes are similar to the holotype, differing sometimes in visibility of bands by having inconspicuous bands that are olive brown [color 278] in QCAZ 8367 to cinnamon drab [color 259] in QCAZ 10614. All specimens present dorsal bands connected on the vertebral axis. Reverse pattern of coloration is also found in this species. Specimens QCAZ 11986, EPN 10548, and EPN 11701 have dorsum of head beige [color 254] followed by a dark grayish brown [color 284] collar; dorsum beige to cinnamon drab [color 259] with dark grayish brown square spots, each covering two scales. Juveniles possess white parietal band and narrow dorsal bands (one-half to one scale long).

Hemipenial morphology (n = 6): Fully everted and maximally expanded hemipenes renders a moderately bilobed (≤ capitulum half length), semicapitate, and semicalyculate organ; lobular region as wide as hemipenial body; lobes centrolinearly oriented, attenuated, conical with acute apices; lobes symmetrical, uniformly covered with spinulate calyces on both sides of hemipenes; spinules replaced with papillae toward apices of lobes; capitular groove distinct on both sides of organ; capitulum with transversal spinulated flounces formed by union of horizontal walls of calyces; calyces lacking vertical walls along the sulcate and asulcate faces of capitulum, except for the intrasulcar region with irregular spinulated flounces; transversal calyculate flounces with irregular rows on the intrasulcar region; flounces conspicuous along lateral region of capitulum; midportion of sulcate face of capitulum with disconnection among transversal flounces; lateral regions of capitulum with regular rows of spinulate calyces; capitulum slightly longer than hempenial body; hemipenial body elliptical covered with enlarged hooked spines; larger spines generally located laterally below sulcus spermaticus bifurcation; distal region of hemipenial body on maximally expanded organ with rows of spines concentrating on the middle of asulcate face; sulcus spermaticus bifurcating approximately at 40% of organ length; sulcus spermaticus margins relatively thick at level of division and along capitular region; sulcus spermaticus not bordered by spinules; basal naked pocket restricted to most basal region of hemipenial body; proximal region of hemipenes body sometimes with shallow groove on the asulcate face, covered with few hooked spines and dispersed spinules; proximal region of hemipenes almost nude (Figure 13).

Quantitative variation (n = 28): Largest female 620 mm SVL, 75 mm TL; largest male 460 mm SVL, 87 mm TL; ventrals 162–175 (mean = 169; n = 3; SD = 6.5) in females, 158–167 (mean = 161; n = 5; SD = 3.6) in males; subcaudals 31–33 (mean = 32; n = 3; SD = 1.1) in females, 39–45 (mean = 43; n = 5; SD = 2.5) in males; supralabials seven (n = 16 sides); infralabials seven (n = 8 sides) or eight (n = 8 sides); preventrals two (n = 2), three (n = 4) or four (n = 2); adult midbody diameter 6.8–8.5 mm; maxillary teeth seven (n = 14 sides).

Distribution: *Atractus pachacamac* inhabits Amazon foothills between 350–1500 m asl from Colombia to Peru, including the surroundings of Sumaco volcano in Ecuador (Figure 14).

Remarks: Camper and Zart (2014) reported earthworms in the diet of this species. After careful examination of museum specimens, we

FIGURE 11 Dorsal (left) and ventral (right) views. Paratypes of *Atractus pachacamac* CORBIDI 167 (a–b) from Güeppi, Maynas, Peru; CORBIDI 13797 (c–d) from Cahuapanas, Datem del Marañón, Peru; QCAZ 8278 (e–f) from Villano, Pastaza, Ecuador. Photos (e–f) by Bioweb/QCAZ

concluded that the specimen listed as *A. touzeti* (ANF 2590 = MZUTI 5409) by Arteaga et al. (2017) belongs to *A. pachacamac*. Furthermore, the specimen referred as *Atractus snethlageae* without voucher, photographed by Arteaga et al. (2017) also is similar to *A. pachacamac*. Thus, as far we know, *A. touzeti* is still known only from its type series from the Cordillera de los Guacamayos in northeastern Ecuador (>1800 m asl; see Schargel et al., 2013 and Passos et al., 2019).

Atractus ***akerios*** **sp. nov.**

urn:lsid:zoobank.org:act:A233B343-8D5E-4DC6-B0F7-98C6E46E17E1

Atractus badius – Cunha and Nascimento (1978), *partim*.

Atractus schach – Cunha and Nascimento (1983); Passos and Fernandes (2008), *partim*; Prudente and Passos (2008), *partim*; Prudente et al. (2018); Cunha and Nascimento (1993).

Atractus snethlageae – Prudente et al. (2018), *partim*.

Holotype: MPEG 12255, adult male from Brazil, Maranhão, Junco do Maranhão, at Nova Vida (1.822°S, 46.109°W), 39 m asl, collected by O.R. da Cunha and F.P. do Nascimento on 1 June 1976.

Paratopotypes (*n* = 4): MPEG 15791, adult female collected on 15 August 1979. MPEG 10347, MPEG 15003, and MPEG 15790, adult males collected by O.R. Cunha and F.P. do Nascimento on 31 October 1975, 1 October 1978, and 15 August 1979.

Paratypes (*n* = 6): Brazil: Pará: Bragança, Bom Jesus (1.077°S, 46.861°W) 44 m asl, MPEG 11374, adult female collected on 7 November 1975; Marabá, São Felix (5.211°S, 49.046°W), 102 m asl, MPEG 11569, MPEG 15165 adult males collected by O.R. Cunha and F.P. do Nascimento on 23 September 1976 and on 15 October 1977; Viseu, Bela Vista (1.444°S, 46.372°W) 21 m asl, MPEG 2295, MPEG 3713, MPEG 10106, adult males collected by O.R. Cunha and F.P. do Nascimento on 21 September 1977, 22 May 1973 and 18 June 1976.

Etymology: The specific epithet "akerios" in the Greek means lifeless. The word is related to the Greek goddess Keres, (Κῆρες) who personifies violent death and destruction. We draw a parallel, where this new species is named after the sudden disappearance in one of the main areas explored and well-studied in relation to Amazonian snakes (see remarks).

Diagnosis: *Atractus akerios* can be distinguished from all congeners by unique combination of the following characters: (1) smooth dorsal scale rows 17/17/17; (2) postoculars two; (3) loreal moderately long; (4) temporal formula 1+2; (5) supralabials usually seven, third and fourth contacting eye; (6) infralabials seven, first four contacting

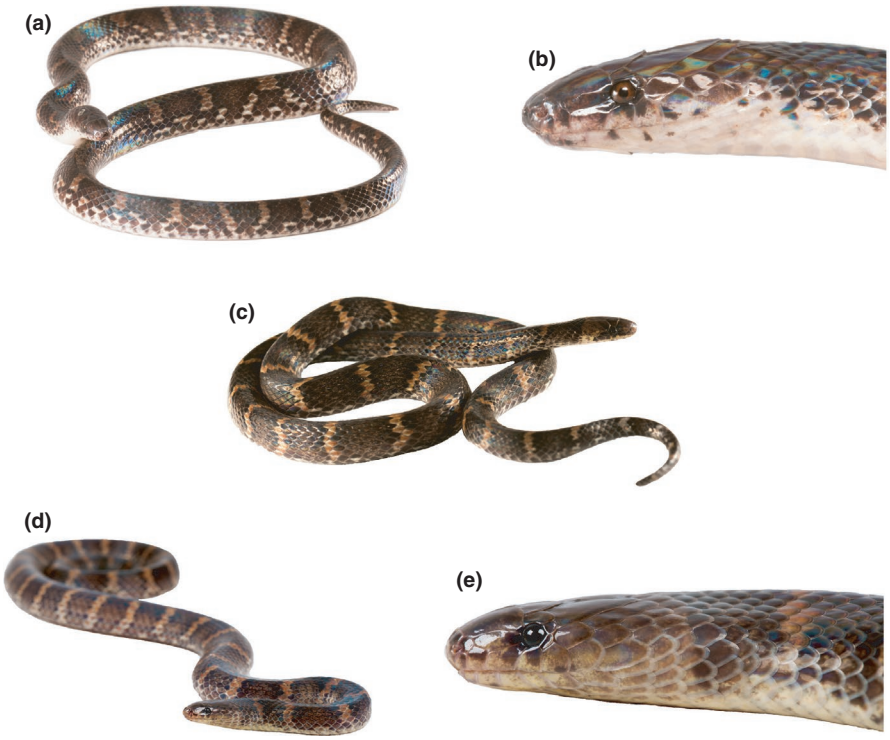

FIGURE 12 Color pattern variation of *Atractus pachacamac*. Holotype: QCAZ 12630 (a–b) from Wildsumaco Wildlife Sanctuary, Napo, Ecuador; Paratypes: QCAZ 15414 (c) from La Zarza, Zamora-Chinchipe, Ecuador; QCAZ 16083 (d–e) from type locality. Photos by Bioweb/QCAZ

chinshields; (7) maxillary teeth usually six; (8) gular scale rows three; (9) usually four preventrals; (10) ventrals 149–156 in females, 140–154 in males; (11) subcaudals 19–20 in females, 24–33 in males; (12) in preservative, dorsum salmon colored to antique brown with russet spots; (13) in preservative, venter sayal brown with Verona brown spots; (14) body moderately long in females (maximum 360 mm SVL) and short in males (290 mm SVL); (15) tail short in females (9.4% of SVL) and moderately long in males (11.7–16.3% of SVL); and (16) hemipenes moderately bilobed (≥half the length of capitulum), semicapitate and semicalyculate.

Comparisons: *Atractus akerios* differs from *A. pachacamac* by having ≤156 ventrals in both sexes, ≤20 and 33 subcaudals in females and males, respectively, and <390 mm of maximum SVL (vs. ≥158 ventrals in both sexes, ≥30 and 39 subcaudals in females and males, respectively, and >400 mm maximum SVL in both sexes); from *A. snethlageae* by having usually four preventrals, 31–56 spots, light dorsal color with small dark spots, ≤20 subcaudals in females, and hemipenes presenting attenuated lobes without lateromesial expansion and with dispersed hooked spines entering the proximal region (vs. frequently three preventrals, 24–34 spots, dorsum Vandyke brown with light yellow ocher bands, ≥21 subcaudals in females, hemipenes presenting flattened, clavated or conical lobes always with lateromesial expansion and organs without hooked spine entering basalmost region); from *A. dapsilis* by having usually four preventrals, 31–56 spots, light dorsal color with small dark spots, ≤20 subcaudals in females, and hemipenes presenting attenuated lobes without laterosmesial expansion and with dispersed hooked spines entering the proximal region (vs. usually three preventrals, 24–34 spots, dorsum sepia with light bands, ≥21 subcaudals in females, hemipenes presenting flattened, clavated or conical lobes always with lateromesial expansion and organs without hooked spine entering basalmost region); from *A. trefauti* by having usually four preventrals, 31–56 spots, light dorsal color with small dark spots, ≤20 subcaudals in females, and hemipenes moderately bilobed without conspicuous capitular groove on both sides (vs. three preventrals, 24–34 spots, dorsum sepia with light bands, ≥21 subcaudals in females, hemipenes slightly bilobed with evident capitular groove on the asulcate side). We refer to Table 1 for additional comparisons between *Atractus akerios* and other Amazonian congeners.

Description of the holotype: SVL 220 mm, tail length 36 mm (16.4% of SVL); head slightly distinct from body; head length 9.7 mm (4.4% of SVL); head width 5.5 mm (56.7% head length); rostral–orbit distance 3.1 mm; nostril–orbit distance 2.25 mm; interorbital distance 3.2 mm; head rounded in lateral view; snout acuminated in dorsal view, truncate in lateral view; canthus rostralis little conspicuous; rostral subtriangular in frontal view, 1.6 mm wide, 0.7 mm high, not visible in dorsal view; internasal 0.8 mm long, 0.9 mm wide; internasal suture sinistral with respect to prefrontal suture; prefrontal 2.0 mm long, 1.7 mm wide; supraocular subtrapezoidal, 0.9 mm long, 0.8 mm wide at broadest point; frontal bell-shaped, 2.6 mm long, 2.6 mm wide; parietal 4.3 mm long, 2.3 mm wide; nasal entirely divided, nostril divided; prenasal 0.8 mm high, 0.4 mm long; postnasal 0.8 mm high, 0.5 mm long; loreal 1.7 mm long, 0.7 mm high; second

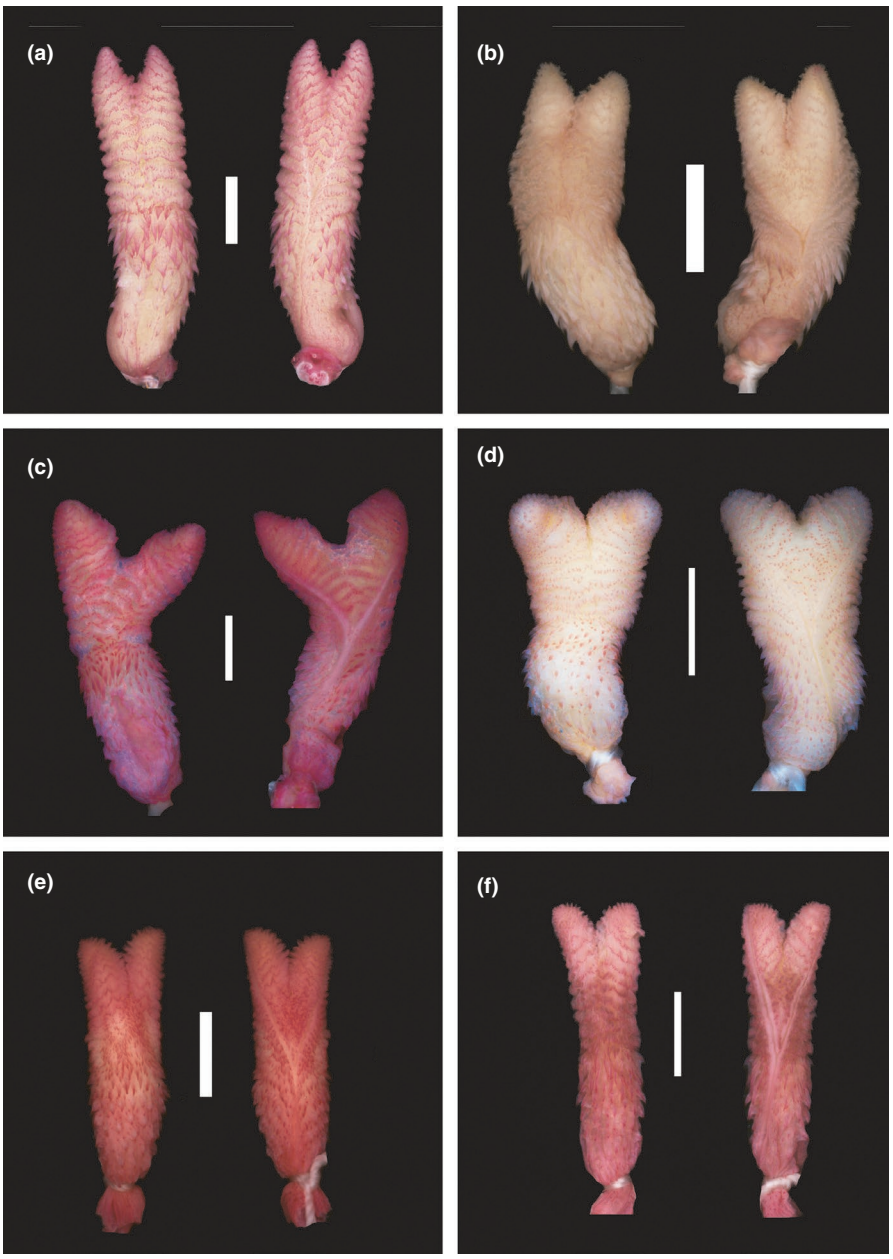

FIGURE 13 Hemipenial morphology of *Atractus pachacamac*. Asulcate (left) and sulcate (right) views of the organs of specimens from Ecuador and Peru: holotype QCAZ 12630 (a), paratype QCAZ 10639 (b), paratype CORBIDI 167 (c), paratype CORBIDI 13797 (d), paratype EPN 5471 (e), and paratype QCAZ 11833 (f) Scale bar = 5 mm

and third supralabials contacting loreal; third and fourth supralabials entering the orbit; eye diameter 1.1 mm; pupil rounded; two postoculars similar in size; upper postocular 0.4 mm long, 0.7 mm high; temporal formula 1+2; first temporal 1.7 mm long, 1.3 mm high; upper posterior temporals 2.9 mm long, 1.1 mm wide; supralabials eight, fourth and fifth contacting eye in the right side; supralabials seven, third and fourth contacting eye in the left side; first supralabial as high (0.9 mm) as second and smaller in length (0.6 mm) than second (0.7 mm); third supralabial pentagonal, larger in height (0.9 mm) and longer (1.1 mm) than second; sixth supralabial taller than third (1.2 mm); seventh as long than sixth (1.7 mm) supralabial; symphysial subtriangular, 1.2 mm wide, 0.4 mm long; first pair of infralabial preventing symphysial–chinshields; infralabials eight, first four contacting chinshields; chinshields 3.0 mm long, 1.2 mm wide; gular scale rows three; preventrals 4; ventrals 143; subcaudals 33 respectively from left to right side; dorsal scale rows 17/17/17, lacking apical pits and supracloacal tubercles; midbody diameter 5.8 mm (2.6% of SVL); caudal spine 0.9 mm long, larger than last subcaudal scale (0.5 mm); anal single. Hemipenes extend at the level of 7th subcaudal. Maxillary bone arched upward anteriorly in lateral view, ventral portion curved on anterior and nearly flattened on median to posterior portion; maxillary with seven teeth; teeth angular in cross section, robust at base, narrower at apices, slightly curved posteriorly; teeth similar in size and spacing; last teeth slightly smaller and in same spacing to anterior

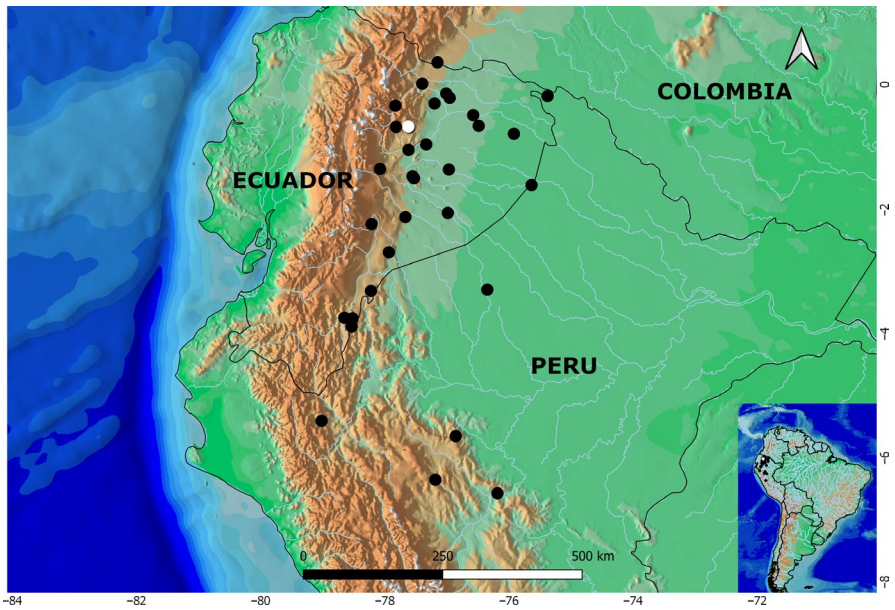

FIGURE 14 Known distribution of *Atractus pachacamac*. Type locality is represented by white dot

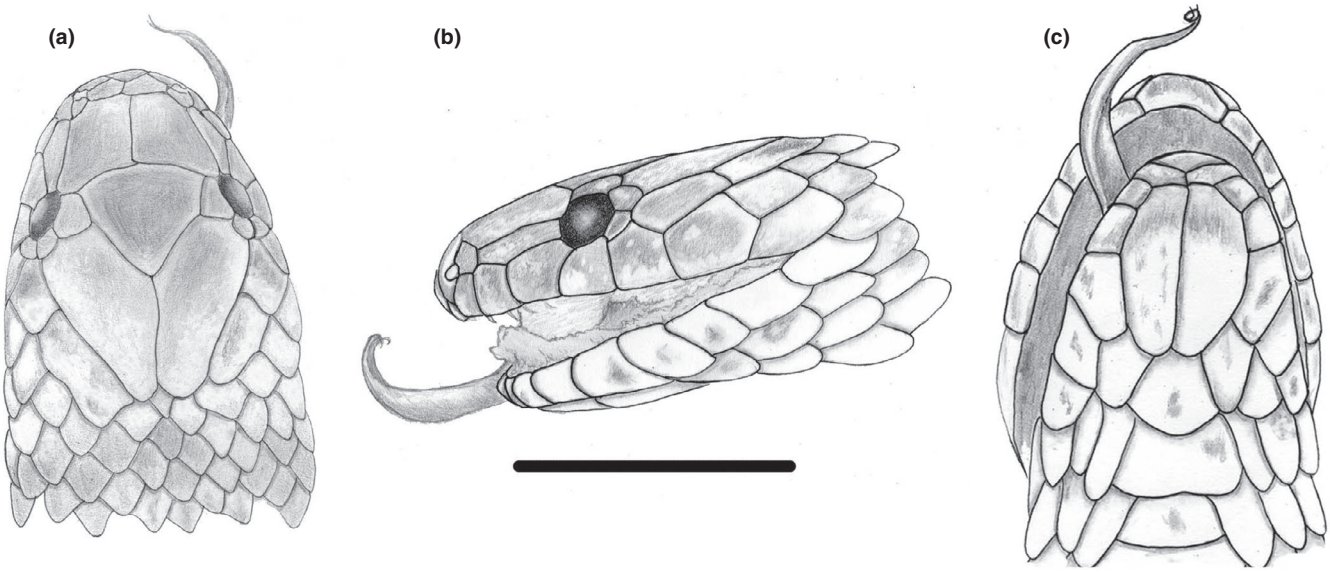

FIGURE 15 Dorsal (a), lateral (b), and ventral (c) views. Holotype of *Atractus akerios* (MPEG 12255) from Nova Vida, Junco do Maranhão, state of Maranhão, Brazil. Scale bar = 5 mm

ones; maxillary "diastema" absent or indistinct from interspaces; lateral process of maxilla well developed.

Dorsum of head antique brown into tip of parietal, where a light occipital band appears being posteriorly bordered by russet collar; lateral of head antique brown covering into sixth supralabial, postoculars and anterior temporal; dorsum salmon to antique brown with russet spots (one or two scales long), light bordered; venter sayal brown with Verona brown spots forming conspicuous midventral line (Figure 15).

Color in life: Unknown.

Color variation (n = 11): The dorsal pattern is quite variable, but predominantly Verona brown to cinnamon, with numerous Burnt umber spots with irregular border, disposed irregularly from the vertebral line until ventral borders. Many specimens show a Raw umber narrow line extending above vertebral axis connecting paravertebral spots; vertebral line most visible on the region posterior to incomplete Raw umber occipital band; anterior part of head Verona brown, followed by incomplete clay collar covering parietals and part of temporals; first four pairs of infralabials and symphysial with irregular Raw umber spots, sometimes extending to chinshields; venter clay color to tawny olive with small Raw umber spots in each scale, extending in a straight line into cloacal plate (Figure 16).

Quantitative variation (n = 10): Largest female 360 mm SVL, 34 mm TL; largest male 290 mm SVL, 43 mm TL; ventrals 149–156

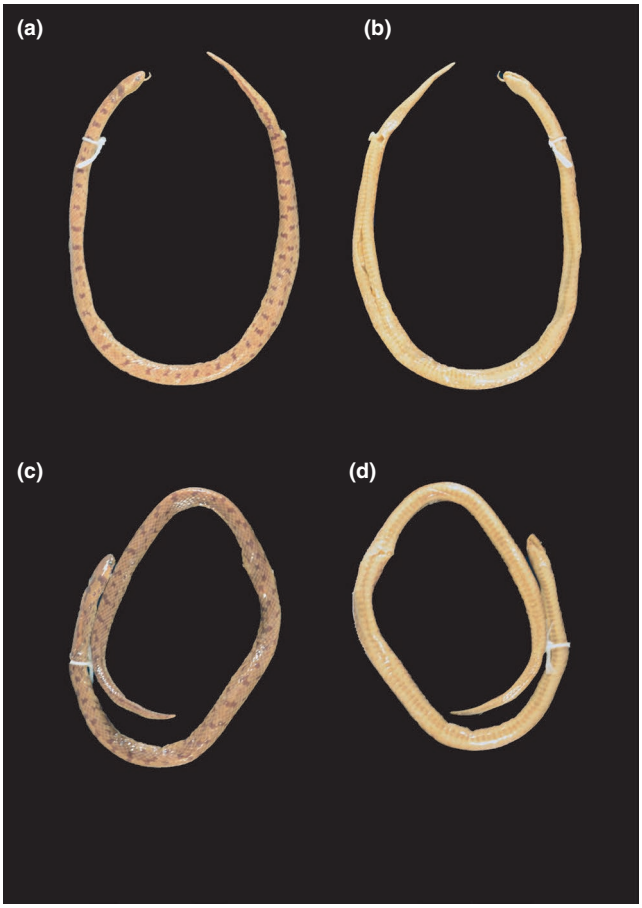

FIGURE 16 Dorsal (left) and ventral (right) views of *Atractus akerios*. Holotype MPEG 12255 (a-b) from Junco do Maranhão, state of Maranhão, Brazil, and paratype MPEG 10106 (c-d) from Viseu, state of Pará, Brazil

(mean = 152.5; *n* = 2; SD = 4.9) in females, 140–154 (mean = 144; *n* = 9; SD = 5.1) in males; subcaudals 19–20 (mean = 19.5; *n* = 2; SD = 0.7) in females, 24–33 (mean = 29.2; *n* = 9; SD = 2.7) in males; supralabials seven (*n* = 23 sides) or eight (*n* = 1 side); preventrals one (*n* = 2), two (*n* = 1), three (*n* = 4) or four (*n* = 5); adult midbody diameter 5.6–7.4 mm; maxillary teeth six (*n* = 18 sides) or seven (*n* = 6 sides).

Hemipenial morphology (*n* = 2): Fully everted and almost maximally expanded hemipenes renders a moderately bilobed (≥ than half capitulum length), semicapitate, and semicalyculate organ; lobular region as wide as hemipenial body; lobes centrolinearly oriented, attenuated with rounded apices; lobes symmetrical; lobes densely covered with spinulate calyces, just above bifurcation of sulcus spermaticus; spinules replaced by irregular papillae toward apices of lobes; capitular groove indistinct on both sides of organ; capitulum with transversal spinulated flounces formed by union of horizontal walls of calyces; calyces lacking vertical walls along the sulcate and asulcate faces of capitulum, except for the intrasulcar region with irregular spinulated flounces; transversal calculate flounces with irregular rows on the intrasulcar region; flounces conspicuous along lateral region of capitulum; midportion of sulcate face of capitulum almost nude by interruption of transversal flounces; lateral regions of capitulum with regular and conspicuous rows of spinulate calyces; hemipenial body elliptical covered with enlarged hooked spines; larger spines generally located laterally below sulcus spermaticus bifurcation; distal region of hemipenial body on maximally expanded organ with rows of spines concentrating on the middle of asulcate face; sulcus spermaticus bifurcates approximately on the 50% of organ length; sulcus spermaticus margins relatively thick at level of division and along the capitular region; sulcus spermaticus narrow, not bordered by spinules; basal naked pocket extending along of hemipenial body, with a large spine in its base; proximal region of hemipenes body covered with few hooked spines and dispersed spinules (Figure 20a).

Distribution: *Atractus akerios* is found in primary forest, except one individual that was found in secondary forest (Cunha & Nascimento, 1983), and is presently known from five sites at extreme eastern portion of the Brazilian Amazonia, one in Junco do Maranhão, state of Maranhão and four in state of Pará between 20–110 m asl (Figure 17).

Remarks: Cunha and Nascimento (1978) reported *Atractus akerios* as *A. badius* from six localities in the state of Pará and one in the state of Maranhão in Brazil. They mentioned color variation ranging from sepia to reddish brown with dark transversal bands, and white or yellowish narrow bands disposed irregularly. Posteriorly, the darker specimens were described as *Atractus flammigerus snethlageae* (Cunha & Nascimento, 1983) whereas the other specimens were associated to *A. schach* (Cunha & Nascimento, 1984) until recently (see Melo-Sampaio et al., 2019). Since we did not obtain new records of specimens collected in the region, the species may have experienced a population decline following changes in land use on this region.

Atractus ***ukupacha*** **sp. nov.**

urn:lsid:zoobank.org:act:C95B553B-1F95-46B5-A73B-4D8AEA48D81D

Atractus snethlageae – Schargel et al. (2013), *partim*; Maynard et al. (2017).

Holotype: QCAZ 12504, adult male from Ecuador, Napo, El Chaco (0.371°S, 77.821°W), 1606 m asl, collected by P. Medrano, on 16 April 2014.

Paratopotype (*n* = 1): QCAZ 4047, adult male collected by R. Cárdenas on 2 November 2006.

Paratypes (*n* = 20): Ecuador: Napo: El Reventador (0.041°S, 77.526°W), 1543 m asl, QCAZ 444, adult female collected by G. Onore on 10 January 1985 and MNRJ 24596 (formerly QCAZ 205) adult male collected by G. Onore on 1 January 1986; San Francisco de Borja (0.424°S, 77.837°W; 1500 m asl), MNRJ 24597, (formerly QCAZ 1320), adult female collected by G. Scacco on 18 April 1992, QCAZ 1606, adult male collected by V. Utreras on 4 January 1992 and QCAZ 12490, adult male collected by P. Medrano on 12 March 2014, QCAZ 12596, adult male by P. Medrano on 17 April 2014 and DHMECN 80, adult male collected by E. Asanza on September 1980; Sardinas (0.340°S, 77.810°W), 1300 m asl, QCAZ 1494, adult female collected by G. Onore on 18 October

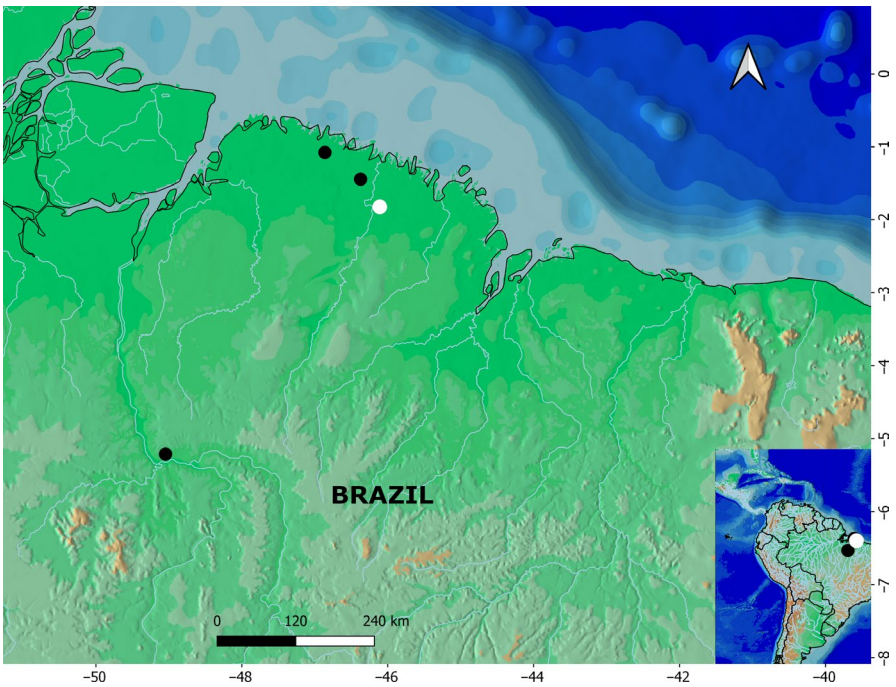

FIGURE 17 Known distribution of *Atractus akerios* in Brazil. The type locality is represented by white dot

1992; Santa Rosa, Quijos (0.394°S, 77.822°W), 1623 m asl, QCAZ 12715, adult female collected by P. Medrano on 24 April 2014. San Rafael, San Rafael stream (0.103°S, 77.580°W), 1190 m asl, QCAZ 0004 and QCAZ 3256, adult males collected by G. Onore on 10 January 1984 and 7 April 1996; Puerto Misahuallí, Reserva Biológica Jatún Sacha (1.050°S, 77.590°W), 406 m asl, QCAZ 3476, adult male and QCAZ 3477 juvenile collected by G. Vigle on 20 September 1986; Cosanga (0.574°S, 77.867°W), 2600 m asl, QCAZ 11202, juvenile collected by E. Tapia on 28 March 1996; Piedra Fina (0.128°S, 77.609°W), 1299 m asl, QCAZ 4812, QCAZ 4942, QCAZ 4943 and QCAZ 4944, juveniles collected by M. Wilkinson on 18 March 2012. Orellana: San José de Payamino (0.464°S, 77.297°W), 370 m asl, QCAZ 11651 and QCAZ 11652, juveniles collected by R. Lynch on 8 June 2013.

Etymology: According to Inca mythology, Uku Pacha represents the underworld, containing the dead and everything that was under terrestrial or aquatic surface. The general legend considers the fountains, caves, volcanoes, and any opening in the Earth's crust as a means of communication between Uku Pacha and Kay Pacha. The word *Pacha* in Quechua Indian language means “time and space”, but into a more general sense means “Earth”. Thus, the specific epithet allows inference to this semi-fossorial lifestyle.

Diagnosis: *Atractus ukupacha* can be distinguished from all congeners by the following combination of characters: (1) smooth dorsal scale rows 17/17/17; (2) postoculars two; (3) loreal moderately long; (4) temporal formula 1+2; (5) supralabials seven, third and fourth contacting eye; (6) infralabials eight, first four contacting chinshields; (7) maxillary teeth seven; (8) gular scale rows three; (9) preventrals two; (10) ventrals 161–170 in females, 153–165 in males; (11) subcaudals 23–33 in females, 38–42 in males; (12) in preservative, dorsum dusky brown with olive-brown bands; (13) in preservative, venter olive-brown with small cream white dots; (14) body moderately long in females (maximum 464 mm SVL) and males (maximum 390 mm SVL); (15) tail moderately long in females (9.9–12.7% of SVL) and long in males (15.5%–20.6% of SVL); and (16) hemipenes strongly bilobed (≥ length of capitulum), semicapitate, and semicalyculate.

Comparisons: *Atractus ukupacha* differs from *A. dapsilis*, *A. schach*, *A. trefauti* by having 161–170 ventrals in females, 153–165 in males, 23–33 subcaudals in females, 38–42 in males, and belly olive-brown with small cream white dots (vs. ventrals 148–150 in females, 142–151 in males, 19–21 subcaudals in females, 25–32 in males of *A. schach*; 30–37 subcaudals in males of *A. dapsilis*; ventrals 153–158 in females, 139–149 in males, 21–24 subcaudals in females, 24–29 in males of *A. trefauti*; and belly mottled in *A. schach* and *A. trefauti*, and cream in *A. dapsilis* usually with brown dots forming an inconspicuous midline); from *A. schach* by having hemipenes with conspicuous capitular groove, 161–170 ventrals in females, 153–165 in males; 23–33 subcaudals in females, 38–42 in males, and tail >15% of SVL in males (vs. hemipenes without capitular groove, 148–150 ventrals in females, 142–151 in males, 19–21 subcaudals in females, 25–32 in males, and tail <15% of SVL in males); from *A. trefauti* by having tail >13.3% of SVL and strongly bilobed hemipenes in males (vs. shorter tail <13.2% and slightly bilobed hemipenes in males); from *A. nawa* by having eight infralabials, and ≥23 subcaudals and >9% of SVL in females (vs. seven infralabials, <21 subcaudals, and tail <9% of SVL in females); from *A. pachacamac* by having spotted preventrals, <500 mm SVL in females, and hemipenes strongly bilobed with lobes centrifugally oriented and flattened on the apices (>600 mm SVL in females, and hemipenes moderately bilobed with lobes centrolineary oriented and attenuated on the apices); from *A. akerios* by having ≥23 and ≥38 subcaudals in females in males, respectively, ≥161 and

153–165 ventrals in females and males respectively, and >390 mm SVL (≤20 and ≤33 subcaudals in females and males, respectively, ≤ 156 and 140–154 ventrals in females and males respectively, and maximum SVL <360 mm); from *A. snethlageae* by lacking light parietal band present >154 ventrals in males, and >38 subcaudals in males (vs. presence of incomplete light parietal band, <154 ventrals and <35 subcaudals in males); from *A. touzeti* by having <700 mm SVL in females, seven supralabials, third and fourth supralabials contacting eye, seven maxillary teeth, postoculars equal in size, and upper and lower posterior temporals equal in size (vs. >700 mm SVL in females, eight supralabials, fourth and fifth supralabials contacting eye, eight maxillary teeth, very small lower postocular, and very large upper posterior temporal). We refer to Table 1 for additional comparisons between *Atractus ukupacha* and other Amazonian congeners.

Description of the holotype: SVL 310 mm, tail length 60 mm (19.3% of SVL); head slightly distinct from body; head length 11.6 mm (3.7% of SVL); head width 7.1 mm (61.2% head length); rostral–orbit distance 4.3 mm; nostril–orbit distance 3.1 mm; interorbital distance 4.3 mm; head rounded in lateral view; snout truncate in dorsal and lateral views; canthus rostralis little conspicuous; rostral subtriangular in frontal view, 2.2 mm wide, 1.1 mm high, well visible in dorsal view; internasal 1.0 mm long, 1.1 mm wide; internasal suture sinistral with respect to prefrontal suture; prefrontal 3.0 mm long, 2.5 mm wide; supraocular subtrapezoidal, 1.5 mm long, 1.3 mm wide at broadest point; frontal bell-shaped, 2.7 mm long, 3.3 mm wide; parietal 4.7 mm long, 3.1 mm wide; nasal entirely divided, nostril divided; prenasal 1.1 mm high, 0.6 mm long; postnasal 1.1 mm high, 0.8 mm long; loreal 2.1 mm long, 0.7 mm high; second and third supralabials contacting loreal; third and fourth supralabials entering the orbit; eye diameter 1.5 mm; pupil rounded; two postoculars distinct in height, with lower shorter than upper; upper postocular 0.7 mm long, 1.0 mm high; lower postocular 0.4 long, 0.7 mm high; temporal formula 1+2; first temporal 1.9 mm long, 1.5 mm high; upper posterior temporals 3.7 mm long, 1.3 mm wide; supralabials seven, third and fourth contacting eye; first supralabial shorter (1.0 mm high) than second (1.4 mm high) and smaller in length (0.6 mm) than second (1.0 mm); third supralabial pentagonal, larger in height (1.5 mm) and longer (1.5 mm) than second; sixth supralabial as tall as third; seventh longer than third (2.5 mm) supralabial; symphysial triangular, 1.7 mm wide, 0.6 mm long; first pair of infralabial preventing symphysial–chinshields; infralabials eight, first four contacting chinshields; chinshields 4.0 mm long, 1.5 mm wide; gular scale rows three; preventral one; ventrals 165; subcaudals 38 respectively from left to right side; dorsal scale rows 17/17/17, lacking apical pits and supracloacal tubercles; midbody diameter 8.5 mm (2.7% of SVL); caudal spine 1.8 mm long, twice larger than last subcaudal scale (0.9 mm). Retracted hemipenes extends to the level of 12th subcaudal, bifurcating at 10th. Maxillary bone arched upward anteriorly in lateral view, ventral portion curved on anterior and nearly flattened on median to posterior portion; maxillary with seven teeth; teeth angular in cross section, robust at base, narrower at apices, slightly curved posteriorly; teeth similar in size and spacing; last teeth slightly smaller and in same spacing to anterior ones; maxillary "diastema" absent; lateral process of maxilla well developed.

Dorsum of head dusky brown through its extension; supralabials and lateral portion of head dusky brown; first four infralabials and gular region olive-brown with burnt umber spots; venter olive-brown with few dispersed cream white dots; lateral portion of ventral scales with cream white spots; ventral surface of tail entirely fuscous; dorsal ground color dusky brown with 33 conspicuous olive-brown bands; interspaces between olive-brown bands 3-5 scales long; first dorsal scale row with light cream, spots in contact with ventral scales forming small line segments; dorsal surface of tail dusky brown with six conspicuous bands; ventral surface of tail fuscous (Figure 18).

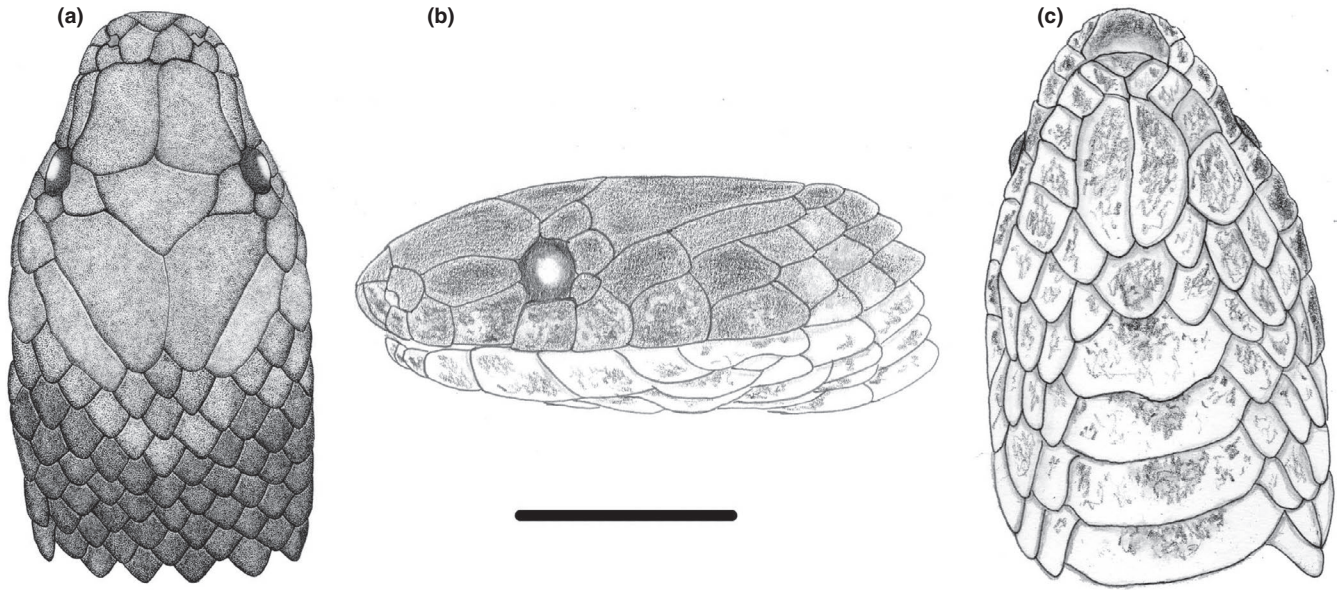

FIGURE 18 Dorsal (a), lateral (b) and ventral (c) views. Holotype of *Atractus ukupacha* (QCAZ 12504) from El Chaco, province of Napo, Ecuador. Scale bar = 5 mm

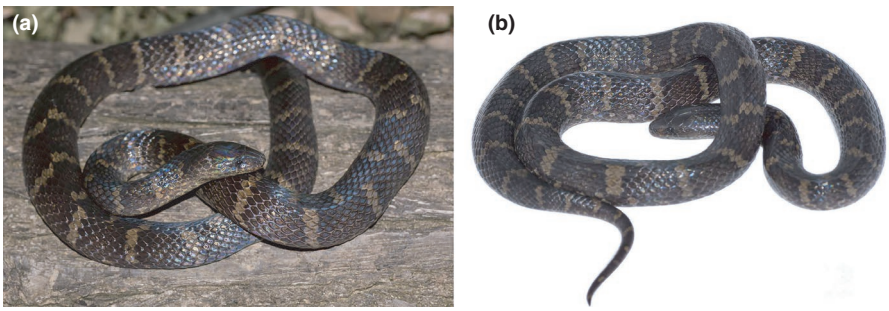

FIGURE 19 Color in life of *Atractus ukupacha*. Uncollected specimen from San José de Payamino, Orellana, Ecuador (a-b). Photos by R. Maynard

Color in life: Dorsum of head dusky brown through its extension; internasals, prefrontals, loreal, supralabials and lateral portion of head dusky brown with orange flecks; first four infralabials and gular region olive-brown with burnt umber spots; dorsal ground color dusky brown with conspicuous olive-brown bands; interspaces between olive-brown bands 3-5 scales long, with tiny orange flecks; first dorsal scale row with light cream, spots in contact with ventral scales forming small line segments (Figure 19).

Color variation (*n* = 17): Dorsum of head olive brown with inconspicuous dark grayish brown [color 284]; dorsum of body sepia to dusky brown [color 285] with dorsal bands varying from pale cinnamon [color 55] to cinnamon [color 21], 1-2 scales long; chinshields, gulars and anterior portion of venter cream suffused with fuscous [color 283] dots; paraventral line connecting light band sometimes present near cloaca. Juveniles present a white parietal band with medial suture diffuse with dark pigments, and dorsal bands two scales long (Figure 19).

Hemipenial morphology (n = 6): Fully everted and almost maximally expanded hemipenes renders a strongly bilobed (≥entire capitulum), semicapitate, and semicalyculate organ; lobular region twice as wide as hemipenial body; lobes centrifugally oriented, clavate with nearly flattened apices on the medial region and laterally conical; lobes uniformly covered with spinulate calyces on both sides of hemipenes; spinules replaced by irregular papillae toward apices of lobes; capitular groove distinct on both sides of organ; capitulum with transversal spinulated flounces formed by union of horizontal walls of calyces; calyces lacking vertical walls along the sulcate and asulcate faces of capitulum, except for the intrasulcar region with irregular spinulated flounces; transversal calyculate flounces with irregular rows on the intrasulcar region; flounces very concentrated and irregular distributed along lateral region of capitulum; high concentration of calyces on the sulcate side of organ sometimes forming longitudinal crests; capitulum slightly shorter than hemipenial body; hemipenial body elliptical covered with enlarged hooked spines; larger spines generally located laterally below sulcus spermaticus bifurcation; distal region of hemipenial body on maximally expanded organ with rows of spines concentrating on the middle of asulcate face; sulcus spermaticus bifurcates approximately on the 50% of organ length; sulcus spermaticus margins relatively thick at the level of division and along the capitular region; sulcus spermaticus not bordered by spinules; basal naked pocket runs beyond sulcus spermaticus bifurcation; proximal region of hemipenes body covered with few hooked spines and dispersed spinules (Figure 20b–f).

Quantitative variation (*n* = 17): Largest female 464 mm SVL, 46 mm TL; largest male 390 mm SVL, 75 mm TL; ventrals 161–170 (mean = 166; *n* = 6; SD = 3.7) in females, 154–165 (mean = 159; *n* = 8; SD = 1.5) in males; subcaudals 23–31 (mean = 27; *n* = 6; SD = 3.6), in females, 38–42 (mean = 39; *n* = 8; SD = 1.5) in males; supralabials seven (*n* = 27 sides), or eight (n = 1 sides); infralabials seven (*n* = 6 sides) or eight (*n* = 22 sides); preventrals two (*n* = 4), three (*n* = 8) or four (*n* = 2).

Distribution: Known from San José de Payamino (370 m asl) to San Franciso de Borja (1744 m asl), Ecuador (Figure 21).

Remarks: Although *Atractus ukupacha* was found in a site near the type locality of *A. touzeti*, they occupy different altitudes (1600 m asl for *A. ukupacha* versus 2200 m asl for *A. touzeti*).

4 | DISCUSSION

We assessed the systematics of the *Atractus snethlageae* complex based on multiple and putatively independent characters (DNA sequences, measurements, scutelation, color pattern, and male genitalia). *Atractus snethlageae* was described as a subspecies of *A. flammigerus* without any evidence of close relationships except for sharing an external banded-pattern. We have recovered here both taxa on distinct clades (Figures S1). Our phylogeny is consistent with a recent study focusing on the *Atractus schach* species complex (Melo-Sampaio et al., 2019). Populations of *Atractus snethlageae* sensu stricto are parapatric with all other species in the complex, except for allopatric *A. ukupacha*. All species were diagnosed upon differences in body size, meristic data, and hemipenial morphology (Figures 5, 13, and 20). Prior to this work, the hemipenis of *A. snethlageae* was never illustrated or even properly described, although this character is very useful for species delimitation (and identification) in the genus *Atractus* (Passos et al., 2018). We describe the male genitalia based on the paratype of *A. snethlageae* (MPEG 10137) and show its variation across its distribution. In this sense, we hope to encourage more descriptions/preparations of this important source of characters for both new and old species.

Although species of the former *A. snethlageae* complex are similar in morphology to other banded species as *A. atlas*, *A. dapsilis*, *A. major*, *A. schach*, *A. touzeti*, and *A. trefauti*, hemipenial morphology markedly differs among them (condition unknown in *A. atlas* and

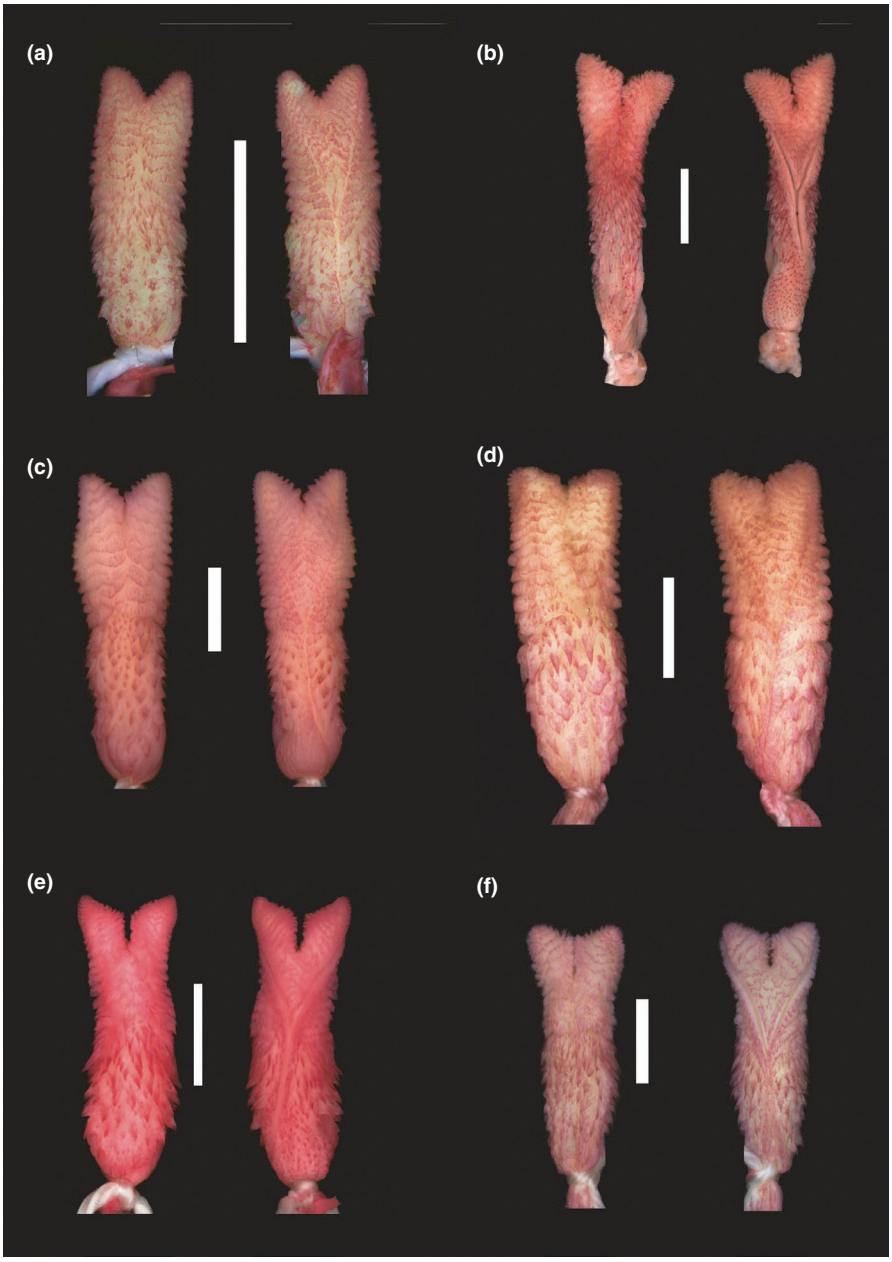

FIGURE 20 Hemipenial morphology. Asulcate (left) and sulcate (right) views of the organs of the holotype of *Atractus akerios* MPEG 12255 (a) from Junco do Maranhão, Maranhão, Brazil; paratypes of *Atractus ukupacha* MNRJ 24596 (formerly QCAZ 205) from El Reventador, Sucumbíos (b), QCAZ 4047 from El Chaco, Napo (c), QCAZ 3476 from Puerto Misahualli, Napo (d), QCAZ 0004 from San Rafael, Napo (f); paratype of *Atractus pachacamac* QCAZ 10614 from Parque Nacional Yasuní, Orellana (e); All from Ecuador. Scale bar = 5 mm

A. touzeti) and molecular data support their recognition as distinct taxa. For example, both *Atractus pachacamac* and *Atractus ukupacha* were sometimes misidentified as *Atractus major*. Both species can be easily diagnosed by the number of infralabials in contact with chinshields. Although *Atractus atlas* and *A. touzeti* also have banded dorsal patterns, they are giant species that differ markedly from *A. snethlageae* complex in scutelation, morphometrics, and coloration. Interestingly, the banded dorsal pattern has evolved multiple times in *Atractus* (e.g., *A. multicinctus* and *A. flammigerus* clades also share this condition). The discovery of additional new species of the *A. snethlageae* complex is expected (see above), especially in Peru and Colombia, where sampling is scanty and diversity is high (see Meneses-Pelayo & Passos, 2019). Further taxonomic studies (using an expanded molecular dataset and hemipenial morphology) are needed to evaluate the status of other related clades.

Atractus akerios, *A. nawa*, and *A. ukupacha* have apparently restricted distributions and probably through denser sampling it is possible to detect other distinct lineages also with narrow ranges of distribution. Many recent studies have pointed that the diversity of the Amazonian herpetofauna is underestimated due to cryptic diversity (Melo-Sampaio et al., 2018, 2019, 2020, 2021; Rojas et al., 2018). The increasing efforts to accurately delimit species in the Neotropics

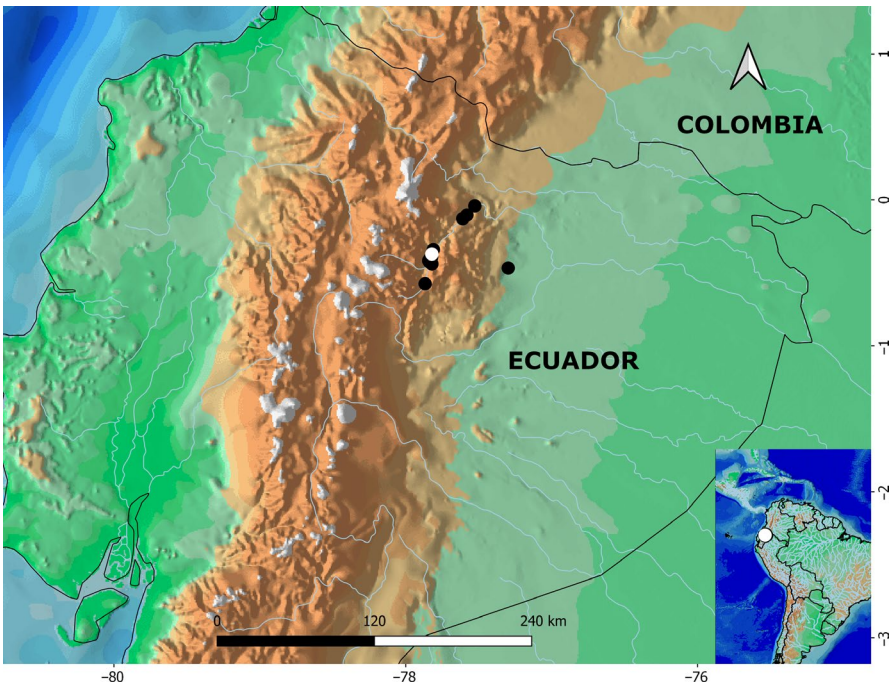

FIGURE 21 Known distribution of *Atractus ukupacha*. Type locality is represented by white dot. Beige areas are above 1000 m asl

have profited from the museum specimens with available tissue samples for molecular studies, allowing falsification of previous hypotheses with premature or misguided taxonomic decisions. We have found a striking diversity of *Atractus* throughout its distribution in the last decade, mostly triggered by the study of a new system of phenotypic characters (Melo-Sampaio et al., 2019; Passos et al., 2017, 2018). On the other hand, many taxa along Amazonian lowlands remain hidden in the shelves of museum collections without proper systematic studies. For example, *Atractus altagratiae* was described only five decades after its own collection event (Passos & Fernandes, 2008), while *A. hoogmoedi* still remained misidentified as *A. zidoki* for ~40 years after the collection of its type specimens (Prudente & Passos, 2010). In the last two decades, herpetological collections from Brazil, Ecuador, and Peru have increased abruptly. Most of these collections come from environmental studies for high-impact projects, allowing biologists to reach to unexplored corners of the Amazon rainforest. In fact, current fieldwork and sampling efforts throughout the Amazonian lowlands is paradoxical, as the best-studied snake faunas are those sampled in the course of "development projects" (e.g., oil exploration, hydroelectric plants, mining, monocultures) that will most likely have a negative impact on biodiversity (Marçal et al., 2011; Morato et al., 2014; Prudente et al., 2010).

We have found areas with high alpha diversity of *Atractus* in both eastern and western extremes of Amazonia. Although we were unable to obtain more tissue samples from western Amazonia (Colombia and Peru), we believe that better sampling including taxa that occur there can improve significantly our understanding of the relationships of *Atractus*. Current documentation of biodiversity is crucial to policies and management of natural resources. Blackburn et al. (2019) show a recent tendency to describe cryptic species using non-morphological (e.g., DNA sequence) data that may impact positively by shortening branch lengths in the tree of life. We highlight that eastern Amazonia is probably the most threatened area of the biome, since 2/3 of its territory has been deforested (Silva et al., 2005; Sonter et al., 2017), although small patches of forest harbor a substantial number of reminiscent snakes (Ávila-Pires et al., 2018). Based on our results and considering previous studies on *Atractus* (Passos et al., 2017, 2018; Prudente & Passos, 2010), at least four species are restricted to this region (i.e., *A. alphonsehogei*, *A. hoogmoedi*, *A. akerios*, and *A. tartarus*), suggesting it should be a relevant conservation area for snakes.

Deforestation in the 21st century has predominantly occurred in the southeastern part of the Amazon, making dry seasons drier and more frequent (Staal et al., 2020); with current deforestation rates, we will face rainfall decreasing up to 20% with consequences in resilience and regrowth (Zemp et al., 2017). Studies in the region are crucial to improve the knowledge about impacts on the biota experiencing fast change on vegetation covering and land use. However, we are just filling some gaps in the knowledge on snake diversity from western Amazonia (Melo-Sampaio et al., 2021; Nogueira et al., 2019).

ACKNOWLEDGMENTS

We thank to Dr. Stephan Koblmüller and two anonymous reviewers for suggestions that improved the manuscript. We are grateful to the following people for allowing us to examine specimens and/or loan tissue samples under their care: C. Aguilar and J. Cordova (MUSM), A. Almendáriz (EPN), J. Aparicio (CBF), M.B. Souza (UFAC-RB), P. Bernarde, R. Machado and L. Turci (UFACF), Y. Bittar (UFPA), J. Lynch and M. Calderón (ICN), P. Campbell (NHM), R. Cassalas and J. Espítia (MLS), F. Curcio (UFMT-R), A. Fouquet (CNRS), F. Franco

and F. Grazziotin (IBSP), L. Gonzalez and R. Montaño (MNK), M. Messias (UNIR), D. Salazar-Valenzuela (MZUTI), J. Valencia (FHGO), W. Vaz (PUC-GO), F. Werneck (INPA), M. Yánez-Muñoz (DHMECN), and H. Zaher (MZUSP). We are deeply indebted to S. Albuquerque, R. Gaiga, R. Lynch, J. López-Rojas, M. Martins, R. Maynard, K. Mebert, D. Meneghelli, L. Moraes, S. Morato, R. Oliveira, U. Oliveira, D. Neira, D. Paiva, M. Pingleton, D. Quirola, D. Rosenberg, W. Vaz and L. Vitt for providing photographs of live specimens. We thank D. Fernandes, R. Fernandes, B. Jennings, and P. Pinna for helpful suggestions on early versions of the manuscript. PRMS thanks L. Lima, K. Silva, and R. Oliveira for friendship and patience during this study. PRMS especially thanks to I. Prates (University of Michigan) for sharing his time and knowledge with prolific discussions and M. T. Rodrigues (USP) for support with workspace, samples, and loan of specimens. PRMS thanks K. de Queiroz, E. Langan, and J. Poindexter (USNM), D.A. Kizirian, L. Vonnnahme (AMNH) for information and photos of specimens under their care. PRMS also acknowledge QCAZ team (Y. Sagredo, M. Stacey, A. Manzano, S. Valverde, F. Ayala-Varela, E. Guerra, V. Chasiluisa, M. Navarrete, G. Maldonado, and S. Guamán), CORBIDI team (J. Chavez-Arribasplata, A. Barbosa), MUSM team (J. Villegas, J. Cusi and G. Gutierrez) for logistic facilities at Quito and Lima, respectively. Financial support for PRMS was provided by Coordenação de Aperfeiçoamento de Pessoal de Nível Superior (CAPES). Financial support for PP was provided by Conselho Nacional de Desenvolvimento Científico e Tecnológico (#309560/2018-7) and Fundação Carlos Chagas Filho de Amparo à Pesquisa do Estado do Rio de Janeiro (#E-26/202.737/2018 and #E-26/211.154/2019). Financial support for ALCP was provided by Conselho Nacional de Desenvolvimento Científico e Tecnológico (#302611/2018-5 and #440413/2015-0). Molecular work and fieldwork by OTC were funded by SENESCYT under the "Arca de Noé" Initiative (PIs: S. Ron and OTC). Fieldwork by PJV were funded by The Field Museum, Chicago.

ORCID

Paulo R. Melo-Sampaio https://orcid.org/0000-0003-1858-1643
Paulo Passos https://orcid.org/0000-0002-1775-0970
Ana L.C. Prudente https://orcid.org/0000-0002-4164-6815
Pablo J. Venegas https://orcid.org/0000-0002-6501-4492
Omar Torres-Carvajal https://orcid.org/0000-0003-0041-9250

REFERENCES

Arteaga, A., Mebert, K., Valencia, J. H., Cisneros-Heredia, D. F., Peñafiel, N., Reyes-Puig, C., Vieira-Fernandes, J. L., & Guayasamin, J. M. (2017). Molecular phylogeny of *Atractus* (Serpentes, Dipsadidae), with emphasis on Ecuadorian species and the description of three new taxa. *ZooKeys*, *661*, 91–123. https://doi.org/10.3897/zookeys.661.11224

Ávila-Pires, T. C. S., Alves-Silva, K. R., Barbosa, L., Correa, F. S., Cosenza, J. F. A., Costa-Rodrigues, A. P. V., Cronemberger, A. A., Hoogmoed, M. S., Lima-Filho, G. R., Maciel, A. O., Missassi, A. F. R., Nascimento, L. R. S., Nunes, A. L. S., Oliveira, L. S., Palheta, G. S., Pereira, A. J. S. Jr, Pinheiro, L., Santos-Costa, M. C., Pinho, S. R. C., … Sturaro, M. J. (2018). Changes in amphibian and reptile diversity over time in Parque Estadual do Utinga, Pará State, Brazil, a protected area surrounded by urbanization. *Herpetology Notes*, *11*, 499–512.

Ávila-Pires, T. C. S., Vitt, L. J., Sartorius, S. S., & Zani, P. A. (2009). Squamata (Reptilia) from four sites in southern Amazonia, with a biogeographic analysis of Amazonian lizards. *Boletim do Museu Paraense Emílio Goeldi Ciências Naturais*, *4*, 99–118.

Bernarde, P. S., & Abe, A. S. (2006). A snake community at Espigão do Oeste, Rondônia, southwestern Amazon, Brazil. *South American Journal of Herpetology*, *1*, 102–113.

Bernarde, P. S., Albuquerque, S., Barros, T. O., & Turci, L. C. B. (2012). Serpentes do estado de Rondônia, Brasil. *Biota Neotropica*, *12*, 154–182.

Bernarde, P. S., Machado, R. A., & Turci, L. C. B. (2011). Herpetofauna of Igarapé Esperança area in the Reserva Extrativista Riozinho da Liberdade, Acre – Brazil. *Biota Neotropica*, *11*, 117–144.

Bernarde, P. S., Turci, L. C. B., & Machado, R. A. (2017). *Serpentes do Alto Juruá: Acre-Amazônia brasileira*. Edufac.

Blackburn, D. C., Giribet, G., Soltis, D. E., & Stanley, E. L. (2019). Predicting the impact of describing new species on phylogenetic patterns. *Integrative Organismal Biology*, *1*, 1–12. https://doi.org/10.1093/iob/obz028

Böhm, M., Collen, B., Baillie, J. E. M., Bowles, P., Chanson, J., Cox, N., Hammerson, G., Hoffmanng, M., Livingstone, S. R., Ram, M., Rhodin, A. G. J., Stuart, S. N., van Dijk, P. P., Young, B. E., Afuang, L. E., Aghasyan, A., García, A., Aguilar, C., Ajtic, R., … Zug, G. (2013). The conservation status of the world's reptiles. *Biological Conservation*, *157*, 372–385. https://doi.org/10.1016/j.biocon.2012.07.015

Boie, F. (1827). Bemerkungen über Merrem's Versuch eines Systems der Amphibien, 1. Lieferung: Ophidier. *Isis Von Oken*, *20*, 508–566.

Boulenger, G. A. (1894). *Catalogue of the snakes in the British Museum (Natural History)*, Vol. *II*. Trustees of the British Museum.

Camper, J. D., & Zart, D. J. (2014). *Atractus snethlageae* (ground snake): diet. *Herpetological Review*, *45*, 705.

Carrillo de Espinoza, N., & Icochea, J. (1995). Lista taxonómica preliminar de los reptiles vivientes del Perú. *Publicaciones Del Museo Historia Natural Universidad Nacioanal Mayor San Marcos*, *47*, 1–27.

Ceballos, G., Ehrlich, P. R., Barnosky, A. D., García, A., Pringle, R. M., & Palmer, T. M. (2015). Accelerated modern human–induced species losses: Entering the sixth mass extinction. *Science Advances*, *1*, e1400253. https://doi.org/10.1126/sciadv.1400253

Cunha, O. R., & Nascimento, F. P. (1978). Ofídios da Amazônia X – As cobras da região leste do Pará. *Publicações Avulsas do Museu Paraense Emílio Goeldi*, *31*, 1–218.

Cunha, O. R., & Nascimento, F. P. (1983). Ofídios da Amazônia XX – As espécies de *Atractus* Wagler, 1828, na Amazônia oriental e Maranhão (Ophidia, Colubridae). *Boletim do Museu Paraense Emílio Goeldi Nova Série Zoologia*, *123*, 1–38.

Cunha, O. R., & Nascimento, F. P. (1984). Ofídios da Amazônia XXI – *Atractus zidoki* no leste do Pará e notas sobre *A. alphonsehogei* e *A. schach*. *Boletim do Museu Paraense Emílio Goeldi Nova Série Zoologia*, *1*, 219–228.

Cunha, O. R., & Nascimento, F. P. (1993). Ofídios da Amazônia X - As cobras da região Leste do Pará. *Boletim do Museu Paraense Emilio Goeldi Nova Série Zoologia*, *9*, 1–191.

de Queiroz, K. (2007). Species concepts and species delimitation. *Systematic Biology*, *56*, 879–886. https://doi.org/10.1080/10635150701701083

Dixon, J. R., & Soini, P. (1986). *The reptiles of the upper Amazon basin, Iquitos region, Peru*. Milwaukee Public Museum.

Doan, T. M., & Arizabal, W. (2000). New herpetological records for the Tambopata Province, Department of Madre de Dios, Peru. *Herpetological Review*, *31*, 188–189.

Doan, T. M., & Arizabal, W. (2002). Microgeographic variation in species composition of the herpetofaunal communities of Tambopata region, Peru. *Biotropica*, *34*, 101–117. https://doi.org/10.1111/j.1744-7429.2002.tb00246.x

Dowling, H. G. (1951). A proposed standard system of counting ventrals in snakes. *British Journal of Herpetology*, *1*, 97–99.

Dowling, H. G., & Savage, J. M. (1960). A guide to snake hemipenis: a survey of basic structure and systematic characteristics. *Zoologica*, *45*, 17–28.

Drummond, A. J., Suchard, M. A., Xie, D., & Rambaut, A. (2012). Bayesian phylogenetics with BEAUti and the BEAST 1.7. *Molecular Biology and Evolution*, *29*, 1969–1973. https://doi.org/10.1093/molbev/mss075

Duellman, W. E. (1978). The biology of an equatorial herpetofauna in Amazonian Ecuador. *Miscellaneous Publication University of Kansas Museum of Natural History*, *65*, 1–352.

Duellman, W. E. (2005). *Cusco Amazónico: the lives of amphibians and reptiles in an Amazonian rainforest*. Cornell University Press.

Duellman, W. E., & Salas, A. W. (1991). Annotated checklist of the amphibians and reptiles of Cuzco Amazónico, Peru. *Occasional Papers of the Museum of Natural History University of Kansas*, *143*, 1–13.

Duméril, A. M. C., Bibron, G., & Duméril, A. H. A. (1854). *Erpétologie générale ou histoire naturelle complète des Reptiles*. Librairie Encyclopédique de Roret.

Ferrer-Paris, J. R., Zager, I., Keith, D. A., Oliveira-Miranda, M. A., Rodríguez, J. P., Josse, C., González-Gil, M., Miller, R. M., Zambrana-Torrelio, C., & Barrow, E. (2019). An ecosystem risk assessment of temperate and tropical forests of the Americas with an outlook on future conservation strategies. *Conservation Letters*, *12*, e12623. https://doi.org/10.1111/conl.12623

Figueroa, A., McKelvy, A. D., Grismer, L. L., Bell, C. D., & Lailvaux, S. P. (2016). A species-level phylogeny of extant snakes with description of a new colubrid subfamily and genus. *PLoS One*, *11*, e0161070. https://doi.org/10.1371/journal.pone.0161070

Fraga, R., Lima, A. P., Prudente, A. L. C., & Magnusson, W. E. (2013). *Guia de cobras da região de Manaus – Amazônia central*. INPA.

Frota, J. G. (2000). Geographic distribution: Serpentes: *Atractus snethlageae*. *Herpetological Review*, *31*, 254.

Frota, J. G. (2004). As serpentes da região de Itaituba, médio rio Tapajós, Pará, Brasil (Squamata). *Comunicações do Museu De Ciências E Tecnologia Da Pontifícia Universidade Católica do Rio Grande do Sul – Série Zoologia*, *17*, 9–19.

Giraudo, A. R. (2004). *Serpientes de la selva paranaense y del Chaco húmedo*. Lola.

Giraudo, A. R., & Scrocchi, G. J. (2000). The genus *Atractus* (Serpentes: Colubridae) in northeastern Argentina. *Herpetological Journal*, *10*, 81–90.

Gonzales, L., & Embert, D. (2008). Geographic distribution: Serpentes: *Atractus snethlageae*. *Herpetological Review*, *39*, 370.

Grazziotin, F. G., Zaher, H., Murphy, R. W., Scrocchi, G., Benavides, M. A., Zhang, Y., & Bonatto, S. L. (2012). Molecular phylogeny of the New World Dipsadidae (Serpentes: Colubroidea): a reappraisal. *Cladistics*, *28*, 1–23. https://doi.org/10.1111/j.1096-0031.2012.00393.x

Gutsche, A., Kwet, A., Kucharzewski, C., Lingnau, R., & Günther, R. (2007). Wilhelm Ehrhardt and an evaluation of his amphibians and reptiles held in the Herpetological Collection of the Museum für Naturkunde, Berlin. *Mitteilungen Aus Dem Museum Für Naturkunde in Berlin Zoologische Reihe*, *83*, 80–93. https://doi.org/10.1002/mmnz.200600019

Hoogmoed, M. S. (1980). Revision of the genus *Atractus* in Surinam, with the ressurection of two species (Colubridae, Reptilia). Notes on the Herpetofauna of Surinam VII. *Zoologische Verhandelingen*, *175*, 1–47.

Hoogmoed, M. S. (1982). Snakes of Guianan region. *Memórias do Instituto Butantã*, *46*, 219–254.

Hoogmoed, M. S., & Prudente, A. L. C. (2003). A new species of *Atractus* (Reptilia: Ophidia: Colubridae: Dipsadinae) from the Amazon forest region in Brazil. *Zoologische Mededelingen*, *77*(15–36), 425–439.

Jorge-da-Silva, N. (1993). The snakes from Samuel hydroelectric power plant and vicinity, Rondônia, Brasil. *Herpetological Natural History*, *1*, 37–86.

Köhler, G. (2012). *Color catalogue for field biologists*. Herpeton.

Kumar, S., Stecher, G., & Tamura, K. (2016). MEGA7: Molecular Evolutionary Genetics Analysis version 7.0 for bigger datasets. *Molecular Biology and Evolution*, *33*, 1870–1874. https://doi.org/10.1093/molbev/msw054

Lanfear, R., Frandsen, P. B., Wright, A. M., Senfeld, T., & Calcott, B. (2016). PartitionFinder 2: new methods for selecting partitioned models of evolution for molecular and morphological phylogenetic analyses. *Molecular Biology and Evolution*, *34*, 772–773. https://doi.org/10.1093/molbev/msw260

Marçal, A. S., Gomes, I. B. R., & Coragem, J. T., (Orgs.). (2011). *UHE Santo Antônio – Guia das espécies de fauna resgatadas*. Scriba Comunicação Corporativa.

Maynard, R., Lynch, R. L., Maier, P., & Hamilton, P. S. (2017). *Reptiles of San José de Payamino, Orellana, Ecuador*. Field Museum.

Melo-Sampaio, P. R., Oliveira, R. M., & Prates, I. (2018). A new nurse frog from Brazil (Aromobatidae: *Allobates*), with data on the distribution and phenotypic variation of Western Amazonian species. *South American Journal of Herpetology*, *13*, 131–149. https://doi.org/10.2994/SAJH-D-17-00098.1

Melo-Sampaio, P. R., Passos, P., Fouquet, A., Prudente, A. L. C., & Torres-Carvajal, O. (2019). Systematic review of *Atractus schach* (Serpentes: Dipsadidae) species complex from the Guiana Shield with description of three new species. *Systematics and Biodiversity*, *17*, 207–229. https://doi.org/10.1080/14772000.2019.1611674

Melo-Sampaio, P. R., Passos, P., Martins, A. R., Jennings, W. B., Moura-Leite, J. C., Morato, S. A. A., Venegas, P. J., Chávez, G., Venâncio, N. M., & Souza, M. B. (2021). A phantom on the trees: Integrative taxonomy supports a reappraisal of rear-fanged snakes classification (Dipsadidae: Philodryadini). *Zoologischer Anzeiger*, *290*, 19–39. https://doi.org/10.1016/j.jcz.2020.10.008

Melo-Sampaio, P. R., Prates, I., Peloso, P. L. V., Recoder, R., Dal Vechio, F., Marques-Souza, S., & Rodrigues, M. T. (2020). A new nurse frog from southwestern Amazonian highlands, with notes on the phylogenetic affinities of *Allobates alessandroi* (Aromobatidae). *Journal of Natural History*, *54*, 43–62. https://doi.org/10.1080/00222933.2020.1727972

Meneses-Pelayo, E., & Passos, P. (2019). New polychromatic species of *Atractus* (Serpentes: Dipsadidae) from the Eastern portion of the Colombian Andes. *Copeia*, *2019*, 250–261. https://doi.org/10.1643/CH-18-163

Montagner, D. (2007). Construção da etnia Náwa. *Revista De Estudos E Pesquisas*, *4*, 33–108.

Montingelli, G. G., Grazziotin, F. G., Battilana, J., Murphy, R. W., Zhang, Y. P., & Zaher, H. (2019). Higher-level phylogenetic affinities of the Neotropical genus *Mastigodryas* Amaral, 1934 (Serpentes: Colubridae), species-group definition and description of a new genus for *Mastigodryas bifossatus*. *Journal of Zoological Systematics and Evolutionary Research*, *57*, 205–239. https://doi.org/10.1111/jzs.12262

Morato, S. A. A., Calixto, P. O., Mendes, L. R., Gomes, R., Galatti, U., Trein, F. L., Oliveira, F. S., & Ferreira, G. N. (2014). *Guia fotográfico de identificação da herpetofauna da Floresta Nacional de Saracá-Taquera, Estado do Pará*. STCP Engenharia de Projetos Ltda.

Nascimento, F. P., Ávila-Pires, T. C., & Cunha, O. R. (1988). Répteis Squamata de Rondônia e Mato Grosso coletados através do Programa Pólo Noroeste. *Boletim do Museu Paraense Emílio Goeldi*, *4*, 21–66.

Nogueira, C. C., Argôlo, A. J. S., Arzamendia, V., Azevedo, J. A., Barbo, F. E., Bérnils, R. S., Bolochio, B. E., Borges-Martins, M., Brasil-Godinho, M., Braz, H., Buononato, M. A., Cisneros-Heredia, D. F., Colli, G. R., Costa, H. C., Franco, F. L., Giraudo, A., Gonzalez, R. C., Guedes, T., Hoogmoed, M. S., … Martins, M. C. M. (2019). Atlas of Brazilian snakes: verified point-locality maps to mitigate the Wallacean shortfall in a megadiverse snake fauna. *South American Journal of Herpetology*, *14*, 1–274. https://doi.org/10.2994/SAJH-D-19-00120.1

Passos, P., Chiesse, A., Torres-Carvajal, O., & Savage, J. (2010). Testing species boundaries within *Atractus occipitoalbus* complex (Serpentes: Dipsadidae). *Herpetologica*, *65*, 384–403. https://doi.org/10.1655/08-024.1

Passos, P., Cisneros-Heredia, D. F., Rivera, D. E., Aguilar, C., & Schargel, W. (2012). Rediscovery of *Atractus microrhynchus* and reappraisal of the taxonomic status of *A. emersoni* and *A. natans* (Serpentes: Dipsadidae). *Herpetologica*, *68*, 375–392. https://doi.org/10.1655/HERPETOLOGICA-D-11-00078.1

Passos, P., Fernandes, D. S., & Borges-Nojosa, D. M. (2007). A new species of *Atractus* (Serpentes: Dipsadinae) from a relictual forest in northeastern Brazil. *Copeia*, *2007*, 788–797.10.1643/0045-8511(2007)7[788:ANSOAS]2.0.CO;2

Passos, P., & Fernandes, R. (2008). A new species of the colubrid snake genus *Atractus* (Reptilia: Serpentes) from the central Amazon of Brazil. *Zootaxa*, *1849*, 59–66. https://doi.org/10.11646/zootaxa.1849.1.4

Passos, P., Fernandes, R., Bérnils, R. S., & Moura-Leite, J. C. (2010). Taxonomic revision of Atlantic Forest *Atractus* (Serpentes: Dipsadidae). *Zootaxa*, *2364*, 1–63. https://doi.org/10.11646/zootaxa.2364.1.1

Passos, P., Kok, P. J. R., Albuquerque, N. R., & Rivas, G. (2013). Groundsnakes of the Lost World: a review of *Atractus* (Serpentes: Dipsadidae) from the Pantepui region, northern South America. *Herpetological Monographs*, *27*, 52–86. https://doi.org/10.1655/HERPMONOGRAPHS-D-12-00001R2.1

Passos, P., Melo-Sampaio, P. R., Ramos, L. O., Grazziotin, F., Fouquet, A., & Torres-Carvajal, O. (in press). When the tail shakes the snake: phylogenetic affinities and morphology of Atractus badius (Serpentes: Dipsadidae), reveals some current pitfalls on the snake's systematics. *Anais da Academia Brasileira de Ciências*.

Passos, P., Mueses-Cisneros, J. J., Lynch, J. D., & Fernandes, R. (2009). Pacific lowland snakes of the genus Atractus (Serpentes: Dipsadidae), with description of three new species. *Zootaxa*, *2293*(1), 1–34. http://dx.doi.org/10.11646/zootaxa.2293.1.1

Passos, P., Prudente, A. L. C., & Lynch, J. D. (2016). Redescription of *Atractus punctiventris* and description of two new *Atractus* (Serpentes: Dipsadidae) from Brazilian Amazonia. *Herpetological Monographs*, *30*, 1–20. https://doi.org/10.1655/HERPMONOGRAPHS-D-14-00009

Passos, P., Prudente, A. L. C., Ramos, L. O., Caicedo-Portilla, J. R., & Lynch, J. D. (2018). Species delimitations in the *Atractus collaris* complex (Serpentes: Dipsadidae). *Zootaxa*, *4392*, 491–520. https://doi.org/10.11646/zootaxa.4392.3.4

Passos, P., Ramos, L. O., Fouquet, A., & Prudente, A. L. C. (2017). Taxonomy, morphology and distribution of *Atractus flammigerus* Boie, 1827 (Serpentes: Dipsadidae). *Herpetologica*, *73*, 349–363. https://doi.org/10.1655/Herpetologica-D-16-00086

Passos, P., Scanferla, A., Melo-Sampaio, P. R., Brito, J., & Almendáriz, A. (2019). A giant on the ground: another large-bodied *Atractus* (Serpentes: Dipsadinae) from Ecuadorian Andes, with comments on the dietary specializations of the goo-eaters snakes. *Anais Da Academia Brasileira De Ciências*, *91*, e20170976. https://doi.org/10.1590/0001-3765201820170976

Pérez-Santos, C. E., & Moreno, A. G. (1988). Ofidios de Colombia. *Museo Regionale Di Scienzi Naturali Torino*, *6*, 6–517.

Pesantes, O. (1994). A method for preparing hemipenis of preserved snakes. *Journal of Herpetology*, *28*, 93–95.

Peters, J. A. (1964). *Dictionary of Herpetology*. Hafner.

Pimm, S. L., Jenkins, C. N., Abell, R., Brooks, T. M., Gittleman, J. L., Joppa, L. N., Raven, P. H., Roberts, C. M., & Sexton, J. O. (2014). The biodiversity of species and their rates of extinction, distribution, and protection. *Science*, *344*, 1246752–1–1246810. https://doi.org/10.1126/science.1246752

Prudente, A. L. C., Maschio, G. F., Santos-Costa, M. C., & Feitosa, D. T. (2010). Serpentes da bacia petrolífera de Urucu, Município de Coari, Amazonas, Brasil. *Acta Amazônica*, *40*, 381–386. https://doi.org/10.1590/S0044-59672010000200016

Prudente, A. L. C., & Passos, P. (2008). A new species of *Atractus* Wagler, 1828 (Serpentes: Dipsadinae) from Guyana plateau in Northern Brazil. *Journal of Herpetology*, *42*, 723–732. https://doi.org/10.1670/07-115R3.1

Prudente, A. L. C., & Passos, P. (2010). New cryptic species of *Atractus* (Serpentes: Dipsadidae) from Brazilian Amazonia. *Copeia*, *2010*, 397–404. https://doi.org/10.1643/CH-08-193

Prudente, A. L. C., & Santos-Costa, M. C. (2005). Checklist of snakes from Ferreira Penna Scientific Station, Eastern Amazonia, Pará State, Brazil. *Boletim do Museu Paraense Emílio Goeldi – Série Ciências Naturais*, *1*, *3*, 203–208.

Prudente, A. L. C., Sarmento, J. F. M., Ávila-Pires, T. C. S., Maschio, G. F., & Sturaro, M. J. (2018). How much do we know about the diversity of Squamata (Reptilia) in the most degraded region of Amazonia? *South American Journal of Herpetology*, *13*, 117–130. https://doi.org/10.2994/SAJH-D-17-00009.1

Pyron, R. A., Arteaga, A., Echevarría, L. Y., & Torres-Carvajal, O. (2016). A revision and key for the tribe Diaphorolepidini (Serpentes: Dipsadidae) and checklist for the genus *Synophis*. *Zootaxa*, *4171*, 293–320. https://doi.org/10.11646/zootaxa.4171.2.4

Pyron, R. A., Burbrink, F. T., & Wiens, J. J. (2013). A phylogeny and revised classification of Squamata, including 4161 species of lizards and snakes. *BioMedCentral Evolutionary Biology*, *13*, 1–53. https://doi.org/10.1186/1471-2148-13-93

Pyron, R. A., Guayasamin, J. M., Peñafiel, N., Bustamante, L., & Arteaga, A. (2015). Systematics of Nothopsini (Serpentes, Dipsadidae), with a new species of *Synophis* from the Pacific Andean slopes of southwestern Ecuador. *ZooKeys*, *541*, 109–147. https://doi.org/10.3897/zookeys.541.6058

Rodrigues, G. M., Maschio, G. F., & Prudente, A. L. C. (2016). Snake assemblages of Marajó Island, Pará state, Brazil. *Zoologia*, *33*, e20150020. https://doi.org/10.1590/S1984-4689zool-20150020

Rodríguez, L. O., & Knell, G. (2004). Amphibians and Reptiles. In: N. Pitman, R. C. Smith, C. Vriesendorp, D. Moskovits, R. Piana, G. Knell, & T. Wachter (Eds.), *Perú: Ampiyacu, Apayacu, Yaguas, Medio Putumayo. Rapid Biological Inventories Report 12* (pp. 152–155). The Field Museum.

Rojas, R. R., Fouquet, A., Ron, S. R., Hernández-Ruz, E. J., Melo-Sampaio, P. R., Chaparro, J. C., Vogt, R. C., Carvalho, V. T., Pinheiro, L. C., Ávila, R. W., Farias, I. P., Gordo, M., & Hrbek, T. (2018). A Pan-Amazonian species delimitation: high species diversity within the genus *Amazophrynella* (Anura: Bufonidae). *PeerJ*, *6*, e4941. https://doi.org/10.7717/peerj.4941

Ronquist, F., Teslenko, M., van der Mark, P., Ayres, D. L., Darling, A., Höhna, S., Larget, B., Liu, L., Suchard, M. A., & Huelsenbeck, J. P. (2012). MrBayes 3.2: Efficient Bayesian phylogenetic inference and model choice across a large model space. *Systematic Biology*, *61*, 539–542. https://doi.org/10.1093/sysbio/sys029

Sabaj, M. (2020). Codes for natural history collections in ichthyology and herpetology. *Copeia*, *108*(3), 593–669. https://doi.org/10.1643/ASIHCODONS2020

Savage, J. M. (1960). A revision of the Ecuadorian snakes of the colubrid genus *Atractus*. *Miscellaneous Publications of the Museum of Zoology University of Michigan*, *112*, 1–86.

Schargel, W. E., Lamar, W. W., Passos, P., Valencia, J. H., Cisneros-Heredia, D. F., & Campbell, J. A. (2013). A new giant *Atractus* (Serpentes: Dipsadidae) from Ecuador, with notes on some other large Amazonian congeners. *Zootaxa*, *3721*, 455–474. https://doi.org/10.11646/zootaxa.3721.5.2

Scheffers, B. R., Oliveira, B. F., Lamb, I., & Edwards, D. P. (2019). Global wildlife trade across the tree of life. *Science*, *366*, 71–76. https://doi.org/10.1126/science.aav5327

Serié, P. (1915). Suplemento a la fauna erpetologica Argentina. *Annales Del Museo Nacional De Historia Natural Buenos Aires*, *27*, 93–109.

Silva, J. M. C., Rylands, A. B., & Fonseca, G. A. B. (2005). The fate of the Amazonian areas of endemism. *Conservation Biology*, *19*, 689–694. https://doi.org/10.1111/j.1523-1739.2005.00705.x

Silva, M. V., Souza, M. B., & Bernarde, P. S. (2012). "2010". Riqueza e dieta de serpentes do Estado do Acre. *Brasil. Revista Brasileira De Zoociências*, *12*, 165–176.

Silva-Haad, J. J. (2004). Las serpientes del género *Atractus* Wagler, 1828 (Colubridae; Xenodontinae) en la Amazonia colombiana. *Revista De La Academia Colombiana De Ciencias Exactas Físicas Y Naturales*, *108*, 409–446.

Sonter, L. J., Herrera, D., Barrett, D. J., Galford, G. L., Moran, C. J., & Soares-Filho, B. S. (2017). Mining drives extensive deforestation in the Brazilian Amazon. *Nature Communications*, *8*, 1013. https://doi.org/10.1038/s41467-017-00557-w

Staal, A., Flores, B. M., Aguiar, A. P. D., Bosmans, J. H. C., Fetzer, I., & Tuinenburg, O. A. (2020). Feedback between drought and deforestation in the Amazon. *Environmental Research Letters*, *15*, 044024. https://doi.org/10.1088/1748-9326/ab738e

Stamatakis, A. (2014). RAxML version 8: a tool for phylogenetic analysis and post-analysis of large phylogenies. *Bioinformatics*, *30*, 1312–1313. https://doi.org/10.1093/bioinformatics/btu033

Stamatakis, A., Hoover, P., & Rougemont, J. (2008). A rapid bootstrap algorithm for the RAxML Web servers. *Systematic Biology*, *57*, 758–771. https://doi.org/10.1080/10635150802429642

Sullivan, J., & Joyce, P. (2005). Model selection in phylogenetics. *Annual Review of Ecology, Evolution and Systematics*, *36*, 445–466. https://doi.org/10.1146/annurev.ecolsys.36.102003.152633

Thompson, J. D., Higgins, D. G., & Gibson, T. J. (1994). CLUSTAL W: improving the sensitivity of progressive multiple sequence alignment through sequence weighting, position-specific gap penalties and weight matrix choice. *Nucleic Acids Research*, *22*, 4673–4680. https://doi.org/10.1007/978-1-4020-6754-9

Torres-Carvajal, O., & Hinojosa, K. C. (2020). Hidden diversity in two widespread snake species (Serpentes: Xenodontini: *Erythrolamprus*) from South America. *Molecular Phylogenetics and Evolution*, *146*, 106772. https://doi.org/10.1016/j.ympev.2020.106772

Uetz, P., Freed, P., & Hošek, J. (Eds.) (2020). *The Reptile Database*. Retrieved from http://www.reptile-database.org

Vaidya, G., Lohman, D. J., & Meier, R. (2011). SequenceMatrix: concatenation software for the fast assembly of multi-gene datasets with character set and codon information. *Cladistics*, *27*, 171–180. https://doi.org/10.1111/j.1096-0031.2010.00329.x

Vanzolini, P. E. (1986a). Addenda and corrigenda to Part I Snakes. In: J. A. Peters, & B. Orejas-Miranda (Eds.), *Catalogue of the Neotropical Squamata. Part I, Snakes*. Smithsonian Institution.

Vanzolini, P. E. (1986b). *Levantamento herpetológico da área do estado de Rondônia sob influência da rodovia BR 364. Relatório de Pesquisa n.1*. MCT/CNPq.

Vaz-Silva, W., Oliveira, R. M., Gonzaga, A. F. N., Pinto, K. C., Poli, F. C., Bilce, T. M., Penhacek, M., Wronski, L., Martins, J. X., Junqueira, T. G., Cesca, L. C. C., Guimarães, V. Y., & Pinheiro, R. D. (2015). Contributions to the knowledge of amphibians and reptiles from Volta Grande do Xingu, northern Brazil. *Brazilian Journal of Biology*, *75*(3), S205–S218. https://doi.org/10.1590/1519-6984.00814BM

Vitt, L. J., Ávila-Pires, T. C. S., Caldwell, J. P., & Oliveira, V. R. L. (1997). The impact of individual tree harvesting on thermal environments of lizards in Amazonian rain forest. *Conservation Biology*, *12*, 654–664. https://doi.org/10.1111/j.1523-1739.1998.96407.x

von May, R., & Mueses-Cisneros, J. J. (2010). Amphibians and Reptiles. In: N. Pitman, C. Vriesendorp, D. K. Moskovits, R. von May, D. Alvira, T. Wachter, D. F. Stotz, & Á. del Campo (Eds.), *Perú: Yaguas-Cotuhé. Rapid Biological Inventories Report 23* (pp. 230–237). The Field Museum.

Waldez, F., Menin, M., & Vogt, R. C. (2013). Diversidade de anfíbios e répteis Squamata na região do baixo rio Purus, Amazônia Central, Brasil. *Biota Neotropica*, *13*, 300–316.

Wilson, E. O. (1988). The current state of biological diversity. In E. O. Wilson, & F. M. Peter (Eds.), *Biodiversity* (pp. 3–18). National Academy Press.

Yánez-Muñoz, M., & Venegas, P. J. (2008). Amphibians and Reptiles. In W. S. Alverson, C. Vriesendorp, Á. del Campo, D. K. Moskovits, D. F. Stotz, M. G. Donayre, & L. A. Borobr (Eds.), *Ecuador-Peru: Cuyabeno-Güeppi, Rapid Biological Inventories Report 20* (pp. 215–221). The Field Museum.

Zaher, H. (1999). Hemipenial morphology of the South American xenodontine snakes, with a proposal for a monophyletic Xenodontinae and a reappraisal of colubroid hemipenes. *Bulletin of the American Museum of Natural History*, *240*, 1–168.

Zemp, D. C., Schleussner, C.-F., Barbosa, H. M. J., & Rammig, A. (2017). Deforestation effects on Amazon forest resilience. *Geophysics Research Letters*, *44*, 6182–6190. https://doi.org/10.1002/2017GL072955

SUPPORTING INFORMATION

Additional supporting information may be found online in the Supporting Information section.

Figure S1. Phylogeny of *Atractus*.

Figure S2. Phylogeny of *Atractus*.

Figure S3. Head of the holotype of *Atractus snethlageae*.

Table S1. Gene regions, primers, and PCR protocols and products used in this study.

Table S2. GenBank accession numbers of sequences used in this work.

Table S3. GenBank sequences excluded from this study with some reidentifications of examined specimens.

Table S4. Partitions and evolutionary models obtained in PartitionFinder2.

Data S1. Alignment.phy. Alignment of three mitochondrial (*16S*, *CYTB*, *ND4*) and three nuclear genes (*CMOS*, *NT3*, *RAG1*) consisting of 3,584 base pairs and 92 terminals used in phylogenetic analyses.

How to cite this article: Melo-Sampaio PR, Passos P, Prudente ALC, Venegas PJ, Torres-Carvajal O. Systematic review of the polychromatic ground snakes *Atractus snethlageae* complex reveals four new species from threatened environments. *J Zool Syst Evol Res*. 2021;59:718–747. https://doi.org/10.1111/jzs.12453

APPENDIX 1

MATERIAL EXAMINED

Specimens marked with asterisk (*) were included in the phylogeny and specimens highlighted in (**bold**) were used to prepare hemipenes. The specimens included in the type series of *Atractus akerios*, *A. nawa*, *A. pachacamac*, *A. snethlageae*, and *A. ukupacha* are not listed again here. Institutional abbreviations follow Sabaj (2020).

***Atractus aboiporu* (*n* = 3)**. Brazil: Amapá: Serra do Navio: (MPEG 25796, holotype; MPEG 25797, paratype); Pedra Branca do Amapari: (MPEG 19783, paratype).

***Atractus* aff. *snethlageae* (*n* = 1)**. Peru: Madre de Díos: Tambopata: CORBIDI 15135*).

***Atractus atlas* (*n* = 4)**. Ecuador: Zamora-Chinchipe: Paquisha: (MEPN 14203, holotype); Parroquía Guayzimi: (DHMECN 2972, paratype). Morona-Santiago: Reserva Biológica Cerro Plateado: (QCAZ 14946*, paratype); Zúñac: (DHMECN 12361, paratype).

***Atractus boimirim* (*n* = 22)**. Brazil: Acre: Cruzeiro do Sul: (UFACF 112). Rondônia: Machadinho d'Oeste (MZUSP 21871, 21983); Samuel Hydroelectric Power Plant at Jamari river: Vila Cachoeira do Samuel: (**MPEG 17908**, holotype; MPEG 17909–11, 17916–17, 17922, 17967–70, paratypes), surroundings of Jaci-Paraná river, tributary of Madeira river: Jirau Hydroelectric Power Plant: (MPEG 23965, paratype), Porto Velho (UFRO-H 45). Pará: Altamira (MZUSP 21716); Juriti: (MNRJ 24864, paratype); Parque Nacional da Amazônia: (MPEG 25259–60, paratypes), Itaituba: (MPEG 21233*).

***Atractus dapsilis* (*n* = 55, including 39 paratypes)**. Brazil: Amazonas: Manaus: (IBSP 49430, IMTM 1061, 1440, INPA-H 18466, 32348, 32271, MZUSP 3713, UFAM 20.06.09); Presidente Figueredo: (IMTM 1354, 1378, 1501, 1563, 1678, MPEG 17426–27, 17495, 17527, 17539, 17559, 17568, MZUSP 8659, 9501). Pará: Oriximiná: (IBSP 87633, MNRJ 14910, **14911**, **14912**, 14913, **14914** [holotype], 14915, 16794*, 16795, 16796*, 16797–801, 16802*, **16804**–03, MPEG 20782, 21569–70, 21712–13, 23505, 23759–60); Terra Santa: (INPA-H 31489, MNRJ 17953–54).

***Atractus flammigerus* (*n* = 3)**. Brazil: Pará: Almeirim (MPEG 21011, 21013, 21353).

***Atractus gigas* (*n* = 17)**. Ecuador: Carchi: km 15 El Chical–Gualtal road, Tulcán Chical: (QCAZ 5771*). Cotopaxi: Bosque Protector Río Guajalito (formerly Palmeras Farm), between San Francisco de Las Pampas and Quito: (FHGO 194, holotype; QCAZ 2099, topotype); Bosque Integral Otonga: (QCAZ 3266), San Francisco de Las Pampas: (QCAZ 175, 179, 443, 647, 662). Pichincha: Cantón San Miguel de los Bancos, Tadayapa road, Tandayapa Farm: (FHGO 4791), Chiriboga: (QCAZ 01), Reserva Las Gralarias: (MZUTI 3286*), Las Palmas: Lloa: (DHMECN 372), Palmeras: (QCAZ 2099), Peñas Coloradas: (QCAZ 4058), Reserva Bella Vista: (QCAZ 6526). Provenance in error: Piso Tropical Oriental: without specific data: (MEPN 8706). Peru: Cajamarca: San Ignacio, Santuario Nacional Tabaconas Namballe: Alto Lhuama: (CORBIDI 877), El Chaupe: (ZFMK 89147).

***Atractus pachacamac* (*n* = 7)**. Colombia: Amazonas: Puerto Nariño (IAVH 3872); Caquetá: Florencia: (MLS 2731). Ecuador: Morona-Santiago: Macas: (EPN 8711). Sucumbios: Lago Agrio: (MECN 7873). Napo: (QCAZ 5074). Peru: Putumayo: Maynas: (MUSM 32287); Andoas: (MUSM 27356). Cajamarca: Jaén: (MUSM 3390).

Atractus schach* (*n* = 12)**. French Guiana: no specific locality: (MNHN 1995.9481, AMNH 139922); Saul: Limonade (**AF1716); Saint-Eugène: (MNHN 1997.2371); Nourágues: (MNHN 2002.615). Guiana: no specific locality (NHM 1939.1.1.95, NHM 1939.1.1.96). Suriname: no specific locality (NHM 1870.3.10.61); Browns Bergen: (RMNH 12683); Petit Saut: (RMNH 38072); Sinnamary river: (SMNS 2664).

***Atractus snethlageae* (*n* = 116)**. Brazil: no specific locality: (MNRJ 9842*). Acre: Marechal Thaumaturgo: (UFAC-RB 227); Cruzeiro do Sul: (UFACF 475). Amazonas: Anamã: (INPA-H 9524); Benjamin Constant: (IBSP 33369); Beruri: (INPA-H 13974–75); Manaus [probably in error] (BMNH 1876.4.23.1). Mato Grosso: Colniza: (UFMT-R **7813**, 7820). Maranhão: Açailândia: (MNRJ 16507); Estreito: (MZUSP 18694). Pará: Altamira: (MZUSP 9334, MPEG 23462); Ananindeua: (MPEG 18518); Barcarena (MPEG 23451); Chaves: (MPEG 24960); Itaituba: (MPEG 21138, 24564, 25149–50); Melgaço: (MPEG 18653, 19863–64, 19966, 19968, 20071, 20605, 21581–83, 23167–68, 23134, 23136); Santarém: (MPEG 19092, 19098); Porto de Moz: (MZUSP 18654–55); Capitão Poço: (MPEG 13267); Vitória do Xingu: (MPEG 19807, 19811, 26191, 26194, 26198–99, 26206, 26208, 26223, 26112, 25834, 25836, 26195, 26203, MNRJ 25233–34, 25239, 24383–85, MZUSP 21769). Rondônia: Ariquemes: (IBSP 41530); Candeias do Jamari: (CHUFC 1399, MPEG 17805–06, 17875–76, 17877–78, 17913–14, 17918–19); Espigão do Oeste: (MPEG 21058); Itapuã do Oeste: (MZUSP 8680); Nova Mamoré: (MPEG 20362); Porto Velho: (INPA-H 27840, 32102, 32372, 34150, 34173, MPEG 23966, 25494–96, MZUSP 19012, 19029–30, 19050–55, 19745, 19985, 20673, UFRO-H 253, 1726–27, 1730, 1732, 1747, 1754, 1757, 2545–2554, 3034–3035, 3725, 3727); Machadinho d'Oeste: (MZUSP 21464–65, 21474, 21862, 21981, **21982**); São Miguel do Guaporé: (MPEG 16554). Peru: Cusco: La Convención: (CORBIDI 10034, 15991, MHNC 48, 182, 377, 422, 424, 1029, MUSM 30847); Madre de Díos: Manu: (MUSM 34987); Tambopata: (CORBIDI 18264). Loreto: Loreto: (IBSP 49431–32); San Martin: Tarapoto: (MUSM 3338). Bolivia: Pando: (MNKR 3275). Colombia: Caquetá: (MLS 140); (ICN 10109–10).

***Atractus tartarus* (*n* = 3)**. Brazil: Pará: (MPEG 25849, MPEG 26456, MPEG 26457).

***Atractus torquatus* (*n* = 4)**. Brazil: Roraima (INPA-H 28565, 28567, 28569, MZUSP 14281). French Guiana: (AF2281).

***Atractus touzeti* (*n* = 3)**. Ecuador: Napo: Cordillera de los Guacamayos: Cosanga–Archidona road: (FHGO 517, holotype); La Virgen: (FHGO 2035–36, paratypes).

Atractus trefauti* (*n* = 6)**. French Guiana: Roura: (**MNRJ 26709, holotype); Mont Tabulaire: (MNHN 2015.56, paratype). Brazil: Amapá: Serra do Navio: (MPEG 25788, MPEG 16382, paratypes); Pará: Almeirim: (MPEG 21354*–55, paratypes).